Journal of Statistical Physics, Vol. 51, Nos. 1/2, 1988

Scaling Laws for Invariant Measures on Hyperbolic and Nonhyperbolic Atractors

P. Grassberger,[1] R. Badii,[2] and A. Politi[3]

Received July 14, 1987

The analysis of dynamical systems in terms of spectra of singularities is extended to higher dimensions and to nonhyperbolic systems. Prominent roles in our approach are played by the generalized partial dimensions of the invariant measure and by the distribution of effective Liapunov exponents. For hyperbolic attractors, the latter determines the metric entropies and provides one constraint on the partial dimensions. For nonhyperbolic attractors, there are important modifications. We discuss them for the examples of the logistic and Hénon map. We show, in particular, that the generalized dimensions have singularities with noncontinuous derivative, similar to first-order phase transitions in statistical mechanics.

KEY WORDS: Dynamical systems; generalized dimensions and entropies; Liapunov exponents; scaling functions; hyperbolicity; phase transitions.

1. INTRODUCTION

The purpose of the present paper is twofold. On one hand, we want to extend the formalism of spectra of singularities[1-3] to higher dimensional strange attractors, i.e., to objects that are not locally isotropic. On the other hand, we discuss the applicability of the thermodynamic approach[4] to nonhyperbolic dynamical systems.

The first problem arises from the fact that strange attractors cannot be completely described by a hierarchy of generalized dimensions,[5-7] but require the concept of "partial dimensions."[8-10] Just as the fractal dimension measures the growth of the mass $p(\varepsilon)$ of an object with its overall size

[1] Physics Department, University of Wuppertal, D-5600, Wuppertal 1, Federal Republic of Germany.
[2] Institute of Theoretical Physics, University of Zurich, CH-8001, Zurich, Switzerland.
[3] Istituto Nazionale di Ottica, I-50125, Firenze, Italy.

0022-4715/88/0400-0135$06.00/0

ε, a partial dimension characterizes the same growth when the size is changed only along one direction. In the context of chaotic dynamical systems, these directions are tangent to the local stable and unstable manifolds.

In the analysis of nonuniform fractals, i.e., those in which the pointwise dimension[11] $\alpha(x)$ assumes more than one value, a scaling function $f(\alpha)$ has been recently introduced[1-3] to characterize the spectrum of "singularities" α. The function $f(\alpha)$ can be interpreted as the Hausdorff dimension of the set of points x with the same pointwise dimension α. An extension of this formalism to nonisotropic fractals is not straightforward, since it is not *a priori* clear whether one should replace $f(\alpha)$ by partial Hausdorff dimensions, or α by partial pointwise dimensions, or both.

Analogously, considering the distribution of orbits in the space of trajectories, instead of the distribution in phase space, it is possible to treat generalized metric entropies by using scaling functions.[12]

Furthermore, both generalized dimensions and entropies can be related to the spectrum of effective Liapunov exponents, which describe the evolution of infinitesimal regions in phase space during a finite amount of time. This allows us to connect static quantities (dimensions) with dynamic quantities (entropies) in some cases, including two-dimensional diffeomorphisms.

In Section 2, generalized dimensions and entropies are defined and the associated scaling functions are introduced. In Section 3, the spectra of effective Liapunov exponents are discussed and related to the quantities defined in Section 2.

The other main purpose of the present paper concerns a problem which is perhaps less elegant but certainly not less important. In fact, practically everything which is known exactly for dissipative chaotic systems only holds for hyperbolic systems. The only notable exception is the class of unimodal maps of an interval onto itself, the best known example of which is the "logistic map"

$$x_{n+1} = 1 - ax_n^2 \tag{1.1}$$

For such transformations, it is known[13] that chaotic orbits exist on sets of parameter values of positive Lebesgue measure. The same is not true, for example, for the Hénon map[14]

$$\begin{aligned} x_{n+1} &= 1 - ax_n^2 + by_n \\ y_{n+1} &= x_n \end{aligned} \tag{1.2}$$

Notice that the logistic map is just the limit $b = 0$. In spite of vast numerical evidence, it is not yet proven rigorously that the transformation (1.2)

indeed possesses a strange attractor, and not just a very long periodic orbit or a very long-lived chaotic transient.

The source of difficulties is the possible occurrence of tangencies between the stable and unstable manifolds (homoclinic tangencies). At such points, the map is not hyperbolic and can be assimilated to the logistic equation (1.1) near the critical point $x=0$, with the attractor corresponding to the parabola $y=1-ax^2$ and the stable manifold corresponding to lines $y=\text{const}$. One effect of the vanishing slope at the critical point of Eq. (1.1) is the existence of a dense set of periodic windows in the logistic map. This is very similar to the Newhouse phenomenon in the Hénon map[15]: even if a chaotic attractor exists at a parameter pair (a, b), there is an infinity of attracting periodic orbits arbitrarily close to it.

Another effect of the critical point in Eq. (1.1) is that the density of the natural measure presents square-root singularities at its forward images. Thus, the dimension function $D(q)$ is not equal to 1 for all values of q, although the natural measure is absolutely continuous, but displays a discontinuity in the derivative at $q=2$ (see also Section 4).[16] In the framework of the thermodynamic formalism,[4] this can be interpreted as a (rather trivial) first-order phase transition. For $q \geqslant 2$, the "phase" consists of the images of the critical point, while for $q<2$, the "normal" points prevail. As a consequence, the formalism developed for hyperbolic systems[4] has to be modified when dealing with nonhyperbolic attractors. Analogously, for the Hénon map, the high-q phase is dominated by the homoclinic tangencies. However, the transition point is no longer at $q=2$.

The logistic equation will be discussed in detail in Section 4 and the Hénon map in Section 5. There, the implications of the nonhyperbolic nature of these systems for the metric entropies are also analyzed.

Before closing the introduction, we should point out that essentially the same problems are expected in other systems with smooth folds of the attractor, such as the Rössler model and the Duffing equation.[17]

2. DIMENSIONS, ENTROPIES, AND SPECTRA OF SINGULARITIES

2.1. Dimensions

Usually, when dealing with fractal objects on which a measure μ is defined, the dimension D is introduced to describe the increase of mass $p(\varepsilon)$ with size ε

$$p(\varepsilon) \sim \varepsilon^D \tag{2.1}$$

In general, however, fractals are nonuniform, i.e., the mss scales differently from point to point. Therefore, one is led to consider pointwise dimensions[11]

$$\alpha(\mathrm{x}) = \lim_{\varepsilon \to 0} \frac{\ln p(\varepsilon, \mathrm{x})}{\ln \varepsilon} \tag{2.2}$$

where $p(\varepsilon, \mathrm{x})$ is the mass of an ε-ball centered at x.

In order to give a global estimate of dimension, it is then necessary to define a suitable average of the "local" dimensions $\alpha(\mathrm{x})$. Originally, the order-q generalized (Renyi) dimensions $D(q)$ were defined as[18,6,7]

$$D(q) = \frac{1}{q-1} \lim_{\varepsilon \to 0} \frac{\ln \sum_i p_i^q(\varepsilon)}{\ln \varepsilon} \qquad \text{for} \quad q \geqslant 0 \tag{2.3}$$

where a regular grid has been chosen and $p_i(\varepsilon)$ is the mass in the ith box. Since the boxes will not be necessarily centered on points of the fractal, some of them will contain spuriously small mass, thus creating problems for negative q values.

For any quantity A_i defined on each box with $p_i \neq 0$, we denote the average ("μ-weighted average") by $\langle A \rangle = \sum_i p_i A_i$. Then, Eq. (2.3) can be written as $\langle p^{q-1} \rangle \sim \varepsilon^{(q-1)D(q)}$. This suggests immediately a more general definition of the dimension function $D(q)$: choose randomly (with respect to the measure μ, not to Lebesgue's measure) domains of size r_i and mass p_i. The dimensions $D(q)$ are then vaguely defined by[8] (see also Ref. 3)

$$\left\langle \left(\frac{p}{r^{D(q)}} \right)^{q-1} \right\rangle \sim \text{const} \qquad \text{for all} \quad r_i \to 0 \tag{2.4}$$

Notice that, for $q \to 0$, this goes over the definition of the Hausdorff dimension, provided that the domains are properly chosen.[8]

Equation (2.4) can be simplified in essentially two complementary ways. In fact, if the result does not depend on the choice of the domains, provided that this is not too unreasonable (as it seems for all applications considered here), we can use balls of fixed radius r centered at randomly chosen points x_i. In this case, Eq. (2.4) reduces to[6,7]

$$\langle\, p(t)^{q-1} \rangle = \int d\mu(\mathrm{x})\, p(r, \mathrm{x})^{q-1} \sim r^{\tau(q)} \qquad \text{for} \quad r \to 0 \tag{2.5}$$

where

$$\tau(q) = (q-1)\, D(q) \tag{2.6}$$

Alternatively, if the measure is sufficiently smooth, one can take balls of equal weight p and variable radii $r_i(p)$ (centered at μ-random x_i). This leads to[19,8]

$$\langle r(p)^{-\tau(q)} \rangle \sim p^{1-q} \qquad \text{for} \quad p \to 0 \tag{2.7}$$

2.2. Spectra of Singularities: Isotropic Case

The characterization of nonuniformity of the previous subsections can be reformulated by introducing a scaling function $f(\alpha)$ describing the spread of values assumed by the pointwise dimension.[1-3] Here, we review that approach, disregarding anisotropy, for later reference.

Since in real calculations limit $\varepsilon \to 0$ cannot be performed, it is useful to consider the ratio

$$\alpha(\varepsilon, x) = \frac{\ln p(\varepsilon, x)}{\ln \varepsilon} \tag{2.8}$$

which we shall call the "crowding index" of the ball centered at the point x, following a suggestion by Kadanoff.[20] We shall also indicate it with the same symbol as the pointwise dimension, since the two quantities coincide in the limit $\varepsilon \to 0$.

Instead of describing nonuniformity through the generalized dimensions $D(q)$, as in Section 2.1, one can proced as follows.[1-3] Introducing the probability density $P(\alpha; \varepsilon)$ of crowding indices

$$P(\alpha; \varepsilon)\, d\alpha = \text{Prob}\{\alpha(\varepsilon, x) \in [\alpha, \alpha + d\alpha]\} \tag{2.9}$$

we can rewrite Eq. (2.5) as

$$\int d\alpha\, P(\alpha; \varepsilon)\, \varepsilon^{(q-1)\alpha} \sim \varepsilon^{\tau(q)} \qquad \text{for} \quad \varepsilon \to 0 \tag{2.10}$$

This scaling law is satisfied by the ansatz[1-3]

$$P(\alpha; \varepsilon) \sim |\ln \varepsilon|^{1/2}\, \varepsilon^{\alpha - f(\alpha)} \tag{2.11}$$

Here, the balls with crowding index α have been chosen according to their own probability. In the limit $\varepsilon \to 0$, the integral is dominated by the value $\alpha(q)$ of α that yields the minimum of the expression $q\alpha - f(\alpha)$. Therefore, one has

$$\tau(q) = \min_{\alpha} \{q\alpha - f(\alpha)\}, \qquad f(\alpha) = \min_{q} \{q\alpha - \tau(q)\} \tag{2.12}$$

i.e., the function $f(\alpha)$ is the Legendre transform of $\tau(q)$. In particular, if $f(\alpha)$ and $\tau(q)$ are differentiable, one gets the relations

$$f(\alpha) = q\alpha(q) - \tau(q), \qquad \alpha(q) = \frac{d\tau(q)}{dq}, \qquad q = \frac{df(\alpha)}{d\alpha} \tag{2.13}$$

We shall continue to write the Legendre tansform in the differential form (2.13), understanding that sometimes it has to be replaced by the more general relations (2.12). If the minima in Eqs. (2.12) are attained at a point in which $f(\alpha)$ is not differentiable, but has finite left and right derivatives, the prefactor $|\ln \varepsilon|^{1/2}$ has to be replaced by $|\ln \varepsilon|$ in Eq. (2.11).

The function $f(\alpha)$ is called the spectrum of crowding indices (or "singularities"). Notice that $\max_\alpha\{f(\alpha)\}$ is the Hausdorff dimension of the (distribution-theoretic) support of μ, while $f(D(1)) = D(1)$ and $f'(D(1)) = 1$, where $D(1)$ is the information dimension.[21] We shall indicate with α^* the value of α where $f(\alpha)$ is maximal, and with $\alpha_{\min}$ ($\alpha_{\max}$) the minimal (maximal) values at which $f(\alpha) \neq -\infty$.

Instead of applying definition (2.5), we could have used relations (2.3) or (2.7) to derive $f(\alpha)$. In the box-counting case [Eq. (2.3)], we have to introduce the probability $\tilde{P}(\alpha; \varepsilon)$ for a randomly chosen box i (of size ε) to have crowding index $\alpha(\varepsilon, \mathrm{x}_i) \in [\alpha, \alpha + d\alpha]$. Here, "random" means with respect to Lebesgue's measure, conditioned on the nonempty boxes, i.e., giving the same weight to all of them. It is easily seen that $\tilde{P}(\alpha; \varepsilon)$ is approximately equal to $P(\alpha; \varepsilon)/[N(\varepsilon)\, p]$, where $N(\varepsilon)$ is the number of nonempty boxes and p is the mass corresponding to that value of α. Since $N(\varepsilon) \sim \varepsilon^{-D(0)}$, we find a scaling ansatz very similar to Eq. (2.11):

$$\tilde{P}(\alpha; \varepsilon) \sim |\ln \varepsilon|^{1/2}\, \varepsilon^{D(0) - f(\alpha)} \tag{2.14}$$

The case of fixed-mass balls is also similar. We now need the probability density $\hat{P}(\alpha; p)$ for the crowding index of a ball of mass p around a point x chosen randomly with respect to μ. With it, Eq. (2.7) reads

$$\int d\alpha\, \hat{P}(\alpha; p)\, p^{-\tau(q)/\alpha} \sim p^{1-q} \qquad \text{for} \quad p \to 0 \tag{2.15}$$

Comparison with Eqs. (2.11), (2.14) shows that

$$\hat{P}(\alpha; p) \sim |\ln p|^{1/2}\, p^{1 - f(\alpha)/\alpha} \tag{2.16}$$

As a result, we can express $f(\alpha)$ in the following three ways:

$$f(\alpha)=\begin{cases}\alpha-\lim\limits_{\varepsilon\to 0}\dfrac{\ln[P(\alpha;\varepsilon)/|\ln\varepsilon|^{1/2}]}{\ln\varepsilon} & \text{(fixed-radius balls)}\\[2ex] D(0)-\lim\limits_{\varepsilon\to 0}\dfrac{\ln[\tilde{P}(\alpha;\varepsilon)/|\ln\varepsilon|^{1/2}]}{\ln\varepsilon} & \text{for } \alpha\leqslant\alpha^* \text{ (box-counting)}\\[2ex] \alpha-\lim\limits_{p\to 0}\dfrac{\alpha\ln[\hat{P}(\alpha;p)/|\ln p|^{1/2}]}{\ln p} & \text{(fixed-mass balls)}\end{cases}\qquad(2.17)$$

Each of these three equations has advantages and drawbacks. First, as we already noted, box counting cannot be used for large α, corresponding to negative q. Second, using balls of fixed radius also creates problems, in practice, for large α: in fact, the measure in these balls is estimated by counting the number of points falling in them; for large α, balls with very low population (and, thus, with very poor statistics) will dominate. This does not affect estimates obtained from fixed-mass balls. There, the corrections due to finite statistics can be estimated exactly for uniform fractal measures and small q (large α).[8] However, the arguments given in Ref. 8 do not seem to hold for strongly nonuniform measures and large q (small α). Hence, we propose to use the first two of equations (2.17) for small α [$\alpha\leqslant D(1)$] and the third one for large α [$\alpha\geqslant D(1)$].

Let us add some remarks about the meaning of $f(\alpha)$: it has been proposed[1,2] to interpret it as the "fractal" dimension of the set of points at which the crowding index is α. This is, however, wrong if one identifies the "fractal" dimension with the box-counting dimension,[5] as is usually done. For instance, for the Feigenbaum attractor, the points with any definite α between $\alpha_{\min}$ and $\alpha_{\max}$ are dense on the attractor[22] and thus the box-counting dimension of any of these sets of points is equal to $D(0)$. Instead, at last in the case of hyperbolic systems, it is true that $f(\alpha)$ is the Hausdorff–Besicovitch dimension of the set of these points.[23] We have thus here the unusual and subtle situation that the fractal dimension does not agree with the Hausdorff dimension, and that the latter is clearly the more relevant. The same will be claimed to occur, in Section 5, for the homoclinic tangency points.

2.3. Partial Dimensions

Strange attractors are, in general, not locally isotropic. A typical example is provided by the generalized baker transformation,[11] which is locally the product of a continuum by a Cantor set. The same holds

roughly also for the Hénon attractor, though it is modified there by singularities building up at forward images of homoclinic tangency points. For a precise characterization of the scaling properties of these sets, we need to generalize the covering procedure, including anisotropic elements like ellipsoids. Accordingly, new parameters have to be introduced, describing the directions of the different axes and the scaling velocity of their lengths. As long as we are interested in the product of fractal sets (defined along preassigned directions) and in the geometrical structure along those directions only, we can confine ourselves to consider ellipsoids of different axes ε_j. In this case, since the probability to fall in a generic ellipsoid factorizes into the product of the probabilities along the local coordinate axes, we can generalize Eq. (2.5) to

$$\langle p(\boldsymbol{\varepsilon})^{q-1} \rangle \sim \prod_{j=1}^{E} \varepsilon_j^{\tau_j(q)} \tag{2.18}$$

with

$$\tau_j(q) = (q-1)\, D_j(q) \tag{2.19}$$

where E is the Euclidean dimension of the space containing the fractal (i.e., the phase space) and the compact vector notation $\boldsymbol{\varepsilon} \equiv (\varepsilon_1, \ldots, \varepsilon_E)$ is used, although it is to be noted that $\boldsymbol{\varepsilon}$ (or $\boldsymbol{\tau}$) is not an element of the tangent space to the phase-space manifold nor of its dual space. The quantities $D_j(q)$ are called (generalized) partial dimensions.[8,10] They sum up to $D(q)$ and are bounded between 0 and 1, for positive values of q:

$$\sum_{j=1}^{E} D_j(q) = D(q) \tag{2.20}$$

$$0 \leqslant D_j(q) \leqslant 1 \qquad \text{for} \quad q \geqslant 0 \tag{2.21}$$

A more general definition, applying to arbitrary fractals, is given in Ref. 8.

2.4. Spectra of Singularities: Anisotropic Case

We shall now discuss the distribution of crowding indices following from the ansatz (2.18). The main problem is to associate a crowding index α to an asymmetric ball. Equation (2.8) cannot be directly applied, since there is no single linear size ε characterizing the ellipsoid. To overcome this difficulty, we write all axes ε_j in terms of a comon length scale ε:

$$\varepsilon_j = \varepsilon^{\eta_j} \tag{2.22}$$

In order to make this equation dimensionally correct, we should write a suitable prefactor s_j, which, for simplicity, will be set numerically to 1, except in Section 3.2. The exponents η_j are positive and can be confined to the interval $[0, 1]$ by setting $\varepsilon \equiv \min\{\varepsilon_1, ..., \varepsilon_E\}$. The usual definition of the isotropic case ($\varepsilon_j = \varepsilon$, $\forall j$) is recovered when $\eta_j = 1$, $\forall j$.

In the general case, with all η's different from 0 or 1, we can formally write

$$p(\boldsymbol{\varepsilon}, \mathrm{x}) \sim \prod_{j=1}^{E} \varepsilon_j^{\alpha_j(\mathrm{x})} \tag{2.23}$$

since we are considering sets which are locally the product of independent structures along the E directions in phase space. The determination of the single α_j's from Eq. (2.23) would require E independent measurements: for each of them, only one axis is let to tend to 0, with the others small enough to be in the asymptotic region. The overall crowding index $\alpha(\varepsilon, \mathrm{x})$, measuring the dependence of p on ε, then depends on the choice of the η_j:

$$\alpha(\varepsilon, \mathrm{x}) = \frac{\ln p(\boldsymbol{\varepsilon}, \mathrm{x})}{\ln \varepsilon} \sim \boldsymbol{\eta} \cdot \boldsymbol{\alpha} \tag{2.24}$$

where $\boldsymbol{\alpha} = (\alpha_1, ..., \alpha_E)$. By introducing, then, the probability density $P(\alpha; \boldsymbol{\varepsilon})$ for finding an index α in an ellipsoid with axes $\boldsymbol{\varepsilon}$, the average (2.18) can be rewritten as

$$\int d\alpha\, P(\alpha; \boldsymbol{\varepsilon}) \boldsymbol{\varepsilon}^{\alpha(q-1)} \sim \varepsilon^{\boldsymbol{\eta} \cdot \boldsymbol{\tau}(q)} \qquad \text{for} \quad \varepsilon \to 0 \tag{2.25}$$

in complete analogy with Eq. (2.10). The generalization of $f(\alpha)$ is straightforward: for any choice of $\boldsymbol{\eta}$, we have a different scaling function $f(\alpha; \boldsymbol{\eta})$, which is the Legendre transform of $\boldsymbol{\eta} \cdot \boldsymbol{\tau}(q)$:

$$\begin{aligned} \alpha(q) &= \boldsymbol{\eta} \cdot \frac{d\boldsymbol{\tau}(q)}{dq} \\ f(\alpha; \boldsymbol{\eta}) &= q\alpha(q) - \boldsymbol{\eta} \cdot \boldsymbol{\tau}(q) = \boldsymbol{\eta} \cdot \left[\frac{d\boldsymbol{\tau}(q)}{dq} q - \boldsymbol{\tau}(q) \right] \end{aligned} \tag{2.26}$$

This implies that both $\alpha(q)$ and $f(\alpha; \boldsymbol{\eta})$ are linear in $\boldsymbol{\eta}$. They can thus be written as

$$\alpha(q) = \boldsymbol{\eta} \cdot \boldsymbol{\alpha} = \sum_{j=1}^{E} \eta_j \alpha_j \qquad \text{with} \quad \alpha_j(q) = d\tau_j(q)/dq \tag{2.27}$$

and

$$f(\alpha; \boldsymbol{\eta}) = \boldsymbol{\eta} \cdot \mathbf{f}(\boldsymbol{\alpha}) \qquad \text{with} \quad f_j = q\alpha_j(q) - \tau_j(q) \tag{2.28}$$

We conjecture that the functions $\alpha_j(q)$ are nothing but the partial pointwise dimensions [introduced in Eq. (2.23)] which dominate the integral in Eq. (2.25) for every given q. Notice, also, that each of the f_j depends only on the corresponding α_j and not on the whole $\boldsymbol{\alpha}$. Moreover, the α_j are not independent of each other, but are functions of the common variable $q = df_j(\alpha_j)/d\alpha_j$. More precisely, let us consider a point x with pointwise dimension $\alpha = \alpha(\mathrm{x})$. From Eq. (2.13), we obtain the value of q for which that pointwise dimension prevails and, from Eq. (2.27), we obtain $\alpha_j = \alpha_j(\mathrm{x})$. The advantage of the above approach is that we never had to deal with the ill-defined partial crowding indices, working always with the overall one, as long as $\varepsilon \neq 0$.

Finally, the distribution of crowding indices satisfies the scaling law

$$P(\alpha; \boldsymbol{\varepsilon}) \sim |\ln \varepsilon|^{1/2} \prod_{j=1}^{E} \varepsilon_j^{\alpha_j - f_j(\alpha_j)} = |\ln \varepsilon|^{1/2}\, \varepsilon^{\boldsymbol{\eta} \cdot (\boldsymbol{\alpha} - \mathbf{f}(\boldsymbol{\alpha}))} \tag{2.29}$$

for $\varepsilon \to 0$, which is the obvious generalization of Eq. (2.11).

The above relations are expected to hold not only for natural measures and not only for attractors, but also for repellers. However, for natural measures on attractors, Eq. (2.29) simplifies considerably, since we expect $D_j(q) = 1$ for j corresponding to unstable directions and for all q, at least for the case of strictly hyperbolic systems we are discussing now. This means that $\alpha_j = 1$ and $f_j(1) = 1$, for the unstable directions [Eq. (2.12) has to be used then, instead of Eq. (2.13)]. As a consequence, the product in Eq. (2.29) can be replaced by a product over the *stable* directions in this case. A further simplification occurs if the Kaplan–York conjecture holds.[24,25] Then, there is only one direction j_0 with $f_{j_0}(\alpha_{j_0}) \neq 0, 1$, and Eq. (2.29) reduces to

$$P(\alpha; \boldsymbol{\varepsilon}) \sim |\ln \varepsilon|^{1/2}\, \varepsilon_{j_0}^{(\alpha_{j_0} - f_{j_0}))}$$

2.5. Generalized Entropies

While generalized dimensions could be defined for any fractal measure, generalized entropies are specific to dynamical systems. We first notice that any invariant measure in phase space also supplies a measure in the space of trajectories. Therefore, rather than averaging masses of balls in phase space, we consider the probability $p(\varepsilon; t)$ of a "sausage" in trajectory space, of spatial size ε and time length t. Quite generally, we expect that[25,26]

$$\left\langle \frac{p(\varepsilon; t)^{q-1}}{\varepsilon^{\tau(q)}} \right\rangle \sim e^{-(q-1)K(q)t} \qquad \text{for} \quad \varepsilon \to 0 \text{ and } t \to \infty \tag{2.30}$$

where ε may or may not be a fluctuating function of the position. As it stands, Eq. (2.30) is somewhat vague, and we shall indeed see later that it is not strictly correct for nonhyperbolic systems. For the moment, we neglect this problem.

Just as in the case of the generalized dimensions, there are (at least) two ways to render Eq. (2.30) more explicit. One consists in taking a fixed grid in trajectory space (i.e., the "sausage" is a cylinder set[27]); the other in averaging over sausages around trajectories chosen randomly with respect to the invariant measure μ.

The second method was effectively used in Refs. 28 and 29 to estimate the metric entropy $K(q=1)$ by computing its lower bound $K(2)$: the number of pairs of orbits remaining closer than ε, during a time t, decreases like $e^{-K(2)t}$

Using a fixed grid is the essence of computing entropies from symbol sequences,. More precisely, we consider symbol sequences obtained by generating partitions. By definition, these are such partitions for which the limit $\varepsilon \to 0$ is not necessary, since it is implied by the limit $t \to \infty$: arbitrarily fine partitions are obtained by intersecting sufficiently many images and preimages of the generator.

Given a symbol sequence $\{..., s_{t-1}, s_t, s_{t+1}, ...\}$, we indicate with $S_t = \{s_1, ..., s_t\}$ a finite subsequence of length t, and call $p\{S_t\}$ the probability to observe S_t at a random position in a very long string (we consider now discrete time, but this is no restriction). The generalized entropies $K(q)$ are then defined as

$$\sum_{\{S_t\}} p\{S_t\}^q \sim e^{(1-q)K(q)t} \qquad \text{for} \quad t \to \infty \tag{2.31}$$

where the sum is performed over all subsequences S_t arising from a generating partition. For a binary partition in which all sequences occur with equal probability, such as for the map $x' = 1 - 2x^2$ (or for the balanced invariant measure on a Julia set), this gives immediately $K(q) = \ln 2$ for all q.

2.6. Crowding in Trajectory Space: Fixed Generators

In analogy with the crowding index in phase space [Eq. (2.8)], let us now define a crowding index

$$\alpha_0(t, S_t) = -\frac{1}{t} \ln p\{S_t\} \tag{2.32}$$

in trajectory space. Here, e^{-t} plays the rôle of ε in Eq. (2.8) and the sequence S_t corresponds to the box i. Furthermore, let us call $\tilde{P}(\alpha_0; t)$ the

probability density for a sequence of length t to have crowding index α_0, once it has been picked randomly among all allowed sequences, independently of their frequency of occurrence. Then, Eq. (2.31) can be written as

$$\int d\alpha_0 \, \tilde{P}(\alpha_0; t) e^{-q\alpha_0 t} \sim e^{-[\tau_0(q) + K(0)]t} \qquad \text{for} \quad t \to \infty \tag{2.33}$$

with $\tau_0(q) = (q-1)\,K(q)$. Comparison with Eq. (2.14) yields immediately the proper scaling law for $\tilde{P}(\alpha_0; t)$ as[12]

$$\tilde{P}(\alpha_0; t) \sim \sqrt{t}\, e^{[f_0(\alpha_0) - K(0)]t} \tag{2.34}$$

with f_0 the Legendre transform of τ_0:

$$\alpha_0(q) = d\tau_0(q)/dq, \qquad f_0(\alpha_0) = q\alpha_0(q) - \tau_0(q) \tag{2.35}$$

As pointed out by Farmer,[30] the mtric entropy can be understood as the information dimension in the space of symbol sequences. Similarly, $f_0(\alpha_0)$ can be interpreted as the Hausdorff dimension of the set of "points" in symbol sequence space with pointwise dimension α_0.[12]

2.7. Crowding in Trajectory Space: No Fixed Generators

Equation (2.30) contains more information than Eq. (2.31), since it yields the simultaneous dependence on t and ε. We shall now use this, by taking sausages around trajectories chosen randomly with respect to μ. Indeed, we shall even go further and consider elliptic cross sections, with axes $\boldsymbol{\varepsilon} = (\varepsilon_1, \ldots, \varepsilon_E)$ directed along the invariant manifolds (stable and unstable). We use the common scale ε as in Eq. (2.22) also for time, by writing

$$\varepsilon_0 \equiv \varepsilon^{\eta_0} = e^{-t} \tag{2.36}$$

Accordingly, we will indicate pointwise entropy and partial dimensions with $\boldsymbol{\alpha} \equiv (\alpha_0, \alpha_1, \ldots, \alpha_E)$, and the size of space-time "balls" (sausages) with $\boldsymbol{\varepsilon} \equiv (\varepsilon_0, \varepsilon_1, \ldots, \varepsilon_E)$. Denoting, then, by $P(\alpha'; \boldsymbol{\varepsilon})$ the probability density to find an overall (i.e., spatiotemporal) crowding index α' [Eqs. (2.8) and (2.32)], we can perform the average (2.30) to obtain

$$\int d\alpha' \, P(\alpha'; \boldsymbol{\varepsilon}) \varepsilon^{\alpha'(q-1)} \sim \boldsymbol{\varepsilon}^{\boldsymbol{\eta} \cdot \boldsymbol{\tau}(q)} \qquad \text{for} \quad \boldsymbol{\varepsilon} \to 0 \tag{2.37}$$

where the first component of $\boldsymbol{\tau}(q)$ is $\tau_0(q) = (q-1)\,K(q)$. Arguments

identical to those of Section 2.4 lead then to a product scaling ansatz completely analogous to Eq. (2.29),

$$P(\alpha'; \varepsilon) \sim |\ln \varepsilon|^{1/2} \prod_{j=0}^{E} \varepsilon_j^{\alpha_j - f_j(\alpha_j)} \qquad \text{for all} \quad \varepsilon_j \to 0 \tag{2.38}$$

We see, thus, that the ansatz (2.30) corresponds to a complete factorization of the probability $p(\varepsilon; t)$ into space and time contributions, except for logarithmic terms. Such a factorization would be obtained if not only the attractor, but also the invariant measure on it were locally a direct product everywhere. There are two subtle points related to that.

The first is that we cannot, in general, expect the attractor to be *topologically* a direct product. Instead, its topological properties can be very different even in simple cases.[31]

The second is that Eq. (2.38) requires more than factorization *nearly* everywhere to be valid. Indeed, if we are interested only in properties holding on sets of measure 1, we could have restricted ourselves to the single value $q = 1$. We see, thus, that we have to be quite careful, since most of rigorously proven theorems only hold for sets of positive measure.

3. EFFECTIVE LIAPUNOV EXPONENTS

3.1. Spectra of Effictive Liapunov Exponents

In Section 2, we dealt with quantities characterizing geometric scaling properties of generic fractal sets. When studying strange attractors, one has the additional information coming from the underlying dynamics, and, in particular, Liapunov exponents can be used to estimate dimensions and metric entropies.[25,32]

In order to study these connections, it is useful to make a distinction similar to that between pointwise dimension [Eq. (2.2)] and crowding index [Eq. (2.8)] for dynamical quantities as well. While Liapunov exponents measure the asymptotic divergence of infinitesimally neighboring trajectories, effective Liapunov exponents refer to large but finite times.[26,33] More precisely, we consider an infinitesimal ball of radius $\varepsilon(\mathrm{x}, t = 0)$, centered at x at time 0. Some time n later (we consider again discrete time), it will be transformed into an ellipsoid with semiaxes $\varepsilon_j(n)$, $j = 1, \ldots, E$. Effective Liapunov exponents are defined as

$$\lambda_j(n, \mathrm{x}) = \frac{1}{n} \lim_{\varepsilon(\mathrm{x},0) \to 0} \ln \frac{\varepsilon_j(n)}{\varepsilon(\mathrm{x}, 0)} \tag{3.1}$$

For strictly hyperbolic systems, this definition is equivalent, as far as applications are concerned, to the following: in each point x, there is an E-bein of tangent vectors $\mathbf{u}_j(\mathrm{x})$ pointing along the invariant manifolds. Calling T the tangent map, we can define effective Liapunov exponents alternatively by

$$\lambda_j(n, \mathrm{x}) = \frac{1}{n} \ln \frac{\|T^n \mathbf{u}_j(\mathrm{x})\|}{\|\mathbf{u}_j(\mathrm{x})\|} \tag{3.2}$$

For nonhyperbolic systems, these two are no longer equivalent. In Sections 4 and 5, we shall use the former definition. It has, e.g., the advantage that for systems with constant Jacobian (such as the Hénon map) the sum of effective Liapunov exponents is also constant, which would not be guaranteed by definition (3.2). Another advantage of (3.1) is that the $\lambda_j(n)$ are ordered according to their magnitude (just as the true Liapunov exponents), while Eq. (3.2) would not preserve the ordering in correspondence of homoclinic tangencies.

In the following, we shall use the vector notation $\boldsymbol{\lambda} = (\lambda_1, ..., \lambda_E)$ without indicating the dependence of $\boldsymbol{\lambda}$ on n. We discuss the distribution $P(\boldsymbol{\lambda}; n)$ of effective Liapunov exponents, in the limit $n \to \infty$, by studying, first, the cumulant generating function $G(n, \mathbf{z})$ defined as

$$G(n, \mathbf{z}) = \ln \int d\mu(\mathrm{x}) \exp[n\mathbf{z} \cdot \boldsymbol{\lambda}(n, \mathrm{x})] \tag{3.3}$$

where $\mathbf{z} = (z_1, ..., z_E)$ is an arbitrary vector with real components. In particular, $G(n, 0) = 0$ and the cumulants of $n\boldsymbol{\lambda}$ are the derivatives of $G(n, \mathbf{z})$ at $\mathbf{z} = 0$. The Liapunov exponents are, finally,

$$\lambda_j = \lim_{n \to \infty} \frac{1}{n} \frac{\partial G(n, \mathbf{z})}{\partial z_j}\bigg|_{\mathbf{z}=0} \tag{3.4}$$

Our essential assumption in the folowing will be that the effective Liapunov exponents, being defined via the logarithms of products of n Jacobi matrices, behave essentially like averages of n random variables correlated only over short times. This leads immediately to the ansatz that $G(n, \mathbf{z})$ depends linearly on n:

$$G(n, \mathbf{z}) \sim n g(\mathbf{z}) \qquad \text{for} \quad n \to \infty \tag{3.5}$$

For the first-order cumulants, this is of course compatible with Eq. (3.4), while for the second-order cumulants, it corresponds to Gaussian central limit behavior. It breaks down only in cases with strong long-time

correlations, as in the case of the intermittent map of Ref. 34 and in area-preserving maps with both regular and irregular regions.[35]

In terms of the probability density $P(\Lambda; n)$ to find effective Liapunov exponents $\lambda(n) \in [\Lambda, \Lambda + d\Lambda]$, the ansatz (3.5) reads, then,

$$\int \prod_{j=1}^{E} d\Lambda_j \, P(\Lambda; n) \exp(n\mathbf{z} \cdot \Lambda) \sim \exp[ng(\mathbf{z})] \qquad \text{for} \quad n \to \infty \tag{3.6}$$

This leads, in a by now standard way, to the following scaling law for $P(\Lambda; n)$,[12]

$$P(\Lambda; n) \sim n^{E/2} \exp[-n\phi(\Lambda)] \qquad \text{for} \quad n \to \infty \tag{3.7}$$

with

$$\phi(\Lambda) = \mathbf{z} \cdot \Lambda(\mathbf{z}) - g(\mathbf{z}) = \max_{\mathbf{z}} \{\mathbf{z} \cdot \Lambda - g(\mathbf{z})\} \tag{3.8}$$

The functions $\Lambda(\mathbf{z})$ and $\mathbf{z}(\Lambda)$ which dominate the integral (3.6) are, then,

$$\Lambda_j(\mathbf{z}) = \frac{\partial g(\mathbf{z})}{\partial z_j} \qquad \text{and, analogously,} \qquad z_j(\Lambda) = \frac{\partial \phi(\Lambda)}{\partial \Lambda_j} \tag{3.9}$$

Notice that the functions Λ_j are mutually independent, just like the z_j, in contrast to the $\alpha_j(q)$.

We shall call the function $\phi(\Lambda)$ the spectrum of effective Liapunov exponents. It is the analog of $\alpha - f(\alpha)$, introduced for crowding indices. In the next two subsections, we shall relate $\phi(\Lambda)$ to the spectra of crowding indices and to generalized dimensions and entropies.

3.2. Relation with Metric Entropies and Partial Dimensions: Global Approach

To derive relations between Liapunov exponents and metric entropies or fractal dimensions one can follow two alternative approaches: a global one, based on implicit expressions for average quantities, or a local one, based on eplicit relations between the corresponding spectra.

In this subsection, we summarize the results of the first approach, indicating its limitations, which are then investigated in Section 3.3.

We first discuss metric entropies, starting from Eq. (2.30), generalized to sausages with arbitrary elliptic cross sections and written as[25,26]

$$\left\langle \frac{p(\boldsymbol{\varepsilon}; t)^{q-1}}{\varepsilon^{\boldsymbol{\eta} \cdot \boldsymbol{\tau}(q)}} \right\rangle \sim e^{-(q-1)K(q)t} \tag{3.10}$$

where the vector notation refers only to the spatial part as in Eq. (2.22), and does *not* include the zeroth component, defined in Eq. (2.36).

The average is taken with respect to μ. We observe that the trajectories remaining for a time t in such a sausage of width ε around $\mathrm{x}(t')$, $t' \in (0,\ t)$, are those that started off in an ellipsoid centered on $\mathrm{x}(0)$ and characterized by $\boldsymbol{\eta}'$ with

$$\eta_j' = \begin{cases} \eta_j - t\lambda_j(t, \mathrm{x})/\ln \varepsilon & \text{if } \lambda_j(t, \mathrm{x}) \geqslant 0 \\ \eta_j & \text{otherwise} \end{cases} \tag{3.11}$$

The probability $p(\boldsymbol{\varepsilon}; t)$ is then equal to the mass $p(\boldsymbol{\varepsilon}'; 0)$ contained in the initial ellipsoid. Hence, inserting Eq. (3.11) into Eq. (3.10), we obtain a statement about the joint distribution of crowding indices and effective Liapunov exponents:

$$\left\langle \frac{p(\boldsymbol{\varepsilon}'; 0)^{q-1}}{\varepsilon^{\boldsymbol{\eta}' \cdot \boldsymbol{\tau}(q)}} \varepsilon^{(\boldsymbol{\eta}' - \boldsymbol{\eta}) \cdot \boldsymbol{\tau}(q)} \right\rangle \sim e^{-(q-1)K(q)t} \tag{3.12}$$

For hyperbolic strange atractors, the crowding index along the expanding directions is not a fluctuating quantity ($\alpha_j = 1$), so that the first term in Eq. (3.12) can be extracted from the brackets. According to Eq. (2.18), such a term is equal to 1, and we obtain[25]

$$\tau_0(q) \equiv (q-1)\, K(q) = -g(1-q, \ldots, 1-q, 0, \ldots, 0) \tag{3.13}$$

where the nonvanishing arguments correspond to the unstable directions. Taking the derivative with respect to q, we obtain from Eq. (3.13)

$$\alpha_0(q) = \sum_{j=1}^{j^+} \Lambda_j(1-q, \ldots, 1-q, 0, \ldots, 0) \tag{3.14}$$

where j^+ is the number of expanding directions. Finally, f_0 can be simply expressed as $f_0(\alpha_0) = \alpha_0(q) - \phi[\boldsymbol{\Lambda}(-\boldsymbol{\tau}_+(q))]$, where $\boldsymbol{\tau}_+(q) = (1-q, \ldots, 1-q, 0, \ldots, 0)$.

While this should hold for hyperbolic attractors, it does not apply to more general systems. First of all, in general (e.g., for strange repellers, for nonhyperbolic attractors, and for nonnatural measures) $\alpha_j \not\equiv 1$ even for the expanding directions. Second, in these cases the left-hand side of Eq. (3.12) cannot in general be factorized for $q \neq 1$. For examples, see the next subsection, Sections 4 and 5, and Ref. 36.

Equation (3.14) generalizes the well-known Pesin formula, which holds for $q = 1$. For $q = 1$, Eq. (3.12) does factorize in all cases discussed above, and we obtain the generalized Pesin formula[37,26,38]

$$K(1) = \sum_{j=1}^{j^+} \lambda_j D_j(1) \tag{3.15}$$

To discuss the relations between Liapunov exponents and fractal dimensions, we start from Eq. (2.18) rewritten in the following form:

$$\left\langle \frac{p(\varepsilon)^{q-1}}{\varepsilon^{\eta \cdot \tau(q)}} \right\rangle \sim 1 \qquad \text{for} \quad \varepsilon \to 0 \tag{3.16}$$

After n iterations, an ellipsoid with axes with axes ε centered at x will be transformed into an ellipsoid with the same mass but with axes

$$\varepsilon_j' = \varepsilon^{\eta_j'} = \varepsilon^{\eta_j} e^{n\lambda_j(\mathbf{x})} \tag{3.17}$$

We assume now that the evolution be invertible, as, e.g., for the Hénon map (but not for the logistic equation). By substituting (3.17) into (3.16) and taking into account the backward invariance of the measure μ, we obtain, then,

$$\left\langle \frac{p(\varepsilon)^{q-1}}{\varepsilon^{\varepsilon \cdot \tau(q)}} \exp[-n\boldsymbol{\lambda} \cdot \tau(q)] \right\rangle \sim 1 \tag{3.18}$$

This relation can be interpreted as a constraint on the partial dimensions $\mathbf{D}(q)$, which has to be satisfied in order to conserve in time the (average) generalized volume at the lhs of Eq. (3.16). It constitutes, essentially, a statement about the joint distribution of crowding indices and expansion rates, the latter evaluated over trajectories starting from the reference ellipsoids. At variance with Eq. (3.12), the first term in Eq. (3.18) also includes contracting directions, for which the partial crowding index is fluctuating. However, for sufficiently large n, we can conjecture that the two quantities become independent for hyperbolic systems, and the average factorizes again. Combining Eqs. (3.18) and (3.16), we obtain the simple relation

$$g(-\tau(q)) = \lim_{n \to \infty} \frac{1}{n} \ln \langle \exp[-n\boldsymbol{\lambda} \cdot \tau(q)] \rangle = 0 \tag{3.19}$$

The existence of correlations between crowding indices and Liapunov exponents will be extensively discussed in the next subsection in terms of local variables. Since Eq. (3.19) constitutes only one constraint on the partial dimensions D_j, it cannot of course determine them univocally. Cases in which all D_j can be explicitly obtained from Eq. (3.19) are two-dimensional maps with constant Jacobian and conformal maps. These will ne discussed in more detail in Section 3.4. In other cases, all D_j are fixed if the Kaplan–Yorke conjecture (see below) is true.

Differentiating Eq. (3.19) with respect to q and using Eqs. (2.13), (3.8), and (3.9), we obtain

$$\sum_{j=1}^{E} \Lambda_j(-\tau(q))\,\alpha_j(q) = 0 \tag{3.20}$$

For $q=1$, the Λ_j are the true Liapunov exponents λ_j and $\alpha_j(1)$ are the partial information dimensions. For this special case, Eq. (3.20) reduces thus to[26,37]

$$\sum_{j=1}^{N} \lambda_j D_j(1) = 0 \tag{3.21}$$

This relation leads immediately to the well-known Kaplan–Yorke formula[24,25] as an *upper bound* on $D(1)$, which was indeed proven rigorously in Ref. 37. As stressed in Ref. 25, relation (3.21) can be interpreted as a conservation equation for the missing information about the actual state of the system: the jth partial dimension is essentially the information density per digit of a coordinate along the jth invariant submanifold, and the Liapunov exponent is the information flow velocity in these digits. Their product is thus a flow rate, and Eq. (3.21) tells us that the divergence of the flow is zero.

For $q \neq 1$, the interpretation of Eq. (3.20) is less straightforward. In the next subsection, the meaning of the functions $\Lambda_j(-\tau(q))$ and $\alpha_j(q)$ will be discussed.

3.3. Local Approach

In the last subsections, we derived global relations for hyperbolic strange attractors under suitable assumptions on factorization of joint probabilities. The main results can be recovered from a purely local approach, which, in addition, allows discussing the role of correlations between dimensions and Liapunov exponents.

The relation between metric entropies and Liapunov exponents can be derived by considering the probability $p(\boldsymbol{\varepsilon}, n, \mathrm{x})$ to find a trajectory that remains for a time n within a sausage of elliptic cross section $\boldsymbol{\varepsilon}$ around the reference orbit starting from x. We assume that $p(\boldsymbol{\varepsilon}, n, \mathrm{x})$ scales, for $n \to \infty$ and $\varepsilon_j \to 0$, as

$$\ln p(\boldsymbol{\varepsilon}, n, \mathrm{x}) \sim \sum_{j=1}^{E} \alpha_j(\mathrm{x}) \ln \varepsilon_j - n\alpha_0(\mathrm{x}) + \text{const} \tag{3.22}$$

where the $\alpha_j(\mathrm{x})$ are the partial pointwise dimensions and $\alpha_0(\mathrm{x})$ is the pointwise entropy.

As in Section 3.2, we again notice that the measure of the sausage is equal to the measure of an ellipsoid around the starting point x, the points of which generate orbits belonging to the sausage: $p(\varepsilon, n, \mathrm{x}) = p(\varepsilon', 0, \mathrm{x})$, where the semiaxes ε_j' are given by Eq. (3.11). Inserting this into Eq. (3.22), the limit $n \to \infty$ and $\varepsilon_j \to 0$ yields

$$\alpha_0(\mathrm{x}) = \sum_{j=1}^{E} \alpha_j(\mathrm{x})\, \lambda_j(\mathrm{x})\, \theta[\lambda_j(\mathrm{x})] \tag{3.23}$$

where θ is the Heaviside function. Notice that both $\alpha_0(\mathrm{x})$ and the $\lambda_j(\mathrm{x})$ refer to the orbit originating from x.

Taking into account that, for the natural measure on hyperbolic attractors, $\alpha_j = 1$ for all expanding directions and all x, we see that Eq. (3.23) is indeed precisely the same as Eq. (3.14). In fact, due to Eq. (2.13), a unique q corresponds to each value of α, while a unique α is attached to each point x. Therefore, we can write $q = q(\mathrm{x})$ and insert it into Eq. (3.14): as a result, we obtain relation (3.23), provided that we identify $\Lambda_j[-\tau_+[q(\mathrm{x})]]$ with $\lambda_j(\mathrm{x})$.

We should point out that Eq. (3.23) holds more generally than for hyperbolic attractors only. In particular, it applies also to repellers, where the $\alpha_j(\mathrm{x})$ are different from 1, along the expanding directions. For one-dimensional repelling maps, one finds

$$\alpha(\mathrm{x}) = [\lambda(\mathrm{x}) - \beta]/\lambda(\mathrm{x}), \qquad \alpha_0(\mathrm{x}) = \alpha(\mathrm{x})\, \lambda(\mathrm{x}) \tag{3.24}$$

with β being the escape rate. The pointwise entropy entropy $\alpha_0(\mathrm{x})$ is thus a product of pointwise dimensions and Liapunov exponents, where the latter are computed over the trajectory starting from x. Therefore, the average (3.12) does not factorize whenever the pointwise dimensions along the expanding directions are not constant. Equation (3.23) can be interpreted as the local counterpart of the Pesin formula (3.15).

The constraint (3.20) on partial dimensions can be obtained by a similar local approach, but more care is required in this case. We use Eq. (3.22) for $n = 0$ and notice, first, that the invariance of the measure implies $p(\varepsilon, \mathrm{x}) = p(\varepsilon', \mathrm{x}')$, with $\mathrm{x}' = F^{(n)}(\mathrm{x})$ and ε_j' given by Eq. (3.17). Furthermore, pointwise dimensions are invariant under the smooth map from x to x'. This is particularly obvious for periodic points, where we can take n as a multiple of the period and obtain the manifestly local version of Eq. (3.20)

$$\sum_{j=1}^{E} \alpha_j(\mathrm{x})\, \lambda_j(\mathrm{x}) = 0 \qquad \text{(periodic points)} \tag{3.25}$$

Again, this should hold more generally than for natural measures on hyperbolic attractors only.

For nonperiodic points, however, the additive constant in Eq. (3.22) cannot be neglected and things are not so easy. While Eq. (3.25) still should hold *nearly* everywhere [since $\lambda_j(\mathrm{x}) = \lambda_j$ nearly everywhere], we could find an everywhere correct local version of Eq. (3.20) only for natural measures on hyperbolic attractors, for which $\alpha_j(\mathrm{x}) = 1$ along all unstable directions. In such a case, we take $\varepsilon_j = O(1)$ for the stable directions and $\varepsilon_j' = O(1)$ for the unstable ones. Taking now the limit $b \to \infty$, with the *end point* x′ kept fixed, we can neglect the additive constant in Eq. (3.22) and obtain

$$\sum_{\text{unstable}} \overleftarrow{\lambda}_j(\mathrm{x}') = -\sum_{\text{stable}} \alpha_j(\mathrm{x}')\, \overleftarrow{\lambda}_j(\mathrm{x}') \tag{3.26}$$

where $\overleftarrow{\lambda}_j(\mathrm{x}) = \lim_{n\to\infty} \lambda_j(\mathrm{x}, -n)$ is the Liapunov exponent of the trajectory leading *to* x, instead of starting *from* x. Equation (3.26) is exactly the same as Eq. (3.20)). We just have to insert $q = q(\mathrm{x}')$ in the latter and identify $\Lambda_j[-\tau[q(\mathrm{x}')]]$ with $\overleftarrow{\lambda}_j(\mathrm{x}')$.

The subtle difference in the argument between Eqs. (3.23) and (3.26) is explicitly verified for the generalized baker transformation[11]

$$(x_{n+1}, y_{n+1}) = \begin{cases} (r_1 x_n,\ y_n/p_1) & \text{if} \quad y_n \leqslant p_1 \\ (r_2 x_n + 1 - r_2,\ (y_n - p_1)/p_2) & \text{if} \quad y_n > p_1 \end{cases} \tag{3.27}$$

with $p_1 + p_2 = 1$ and $r_1 + r_2 < 1$. A trajectory of this map can be encoded by the symbol sequence $\{\sigma_n \mid n = 0, \pm 1, \pm 2, \ldots\}$, where

$$\sigma_n = \mathrm{sgn}(y_n - p_1) \tag{3.28}$$

The natural measure is such that the sequence of symbols is uncorrelated with $\mathrm{prob}(\sigma = -1) = p_1$ and $\mathrm{prob}(\sigma = +1) = p_2$. The partial dimension α_2 at the point x_n is a function of σ_k with $k < n$ only, while $\alpha_1 = 1$. The effective Liapunov exponents $\lambda_j(\mathrm{x}_m, n)$ depend only on the σ_k with $m \leqslant k < n + m$. A thin horizontal strip around x_m of height $\Delta y = \exp[-n\lambda_1(\mathrm{x}_m, n)]$ and width $\Delta x = 1$ is mapped, after n iterations, onto a thin vertical strip with $\Delta y = 1$ and $\Delta x = \exp[n\lambda_2(\mathrm{x}_m, n)]$. Conservation of probability, together with Eq. (2.2), yields

$$\alpha_2(\mathrm{x}_{m+n}) = -\lambda_1(\mathrm{x}_m, n)/\lambda_2(\mathrm{x}_m, n) \tag{3.29}$$

Taking the limit $n \to \infty$, we obtain indeed Eq. (3.26). The partial pointwise dimension along the contracting direction depends on the Liapunov exponents computed over the past history of the point, at variance with

partial dimensions along expanding directions (see the case of repellers), which depend on "future" values of the Liapunov exponents. This justifies the assumption of factorization after Eq. (3.18): the first factor in brackets depends on $\alpha_2(x)$, which is a function of "old" Liapunov exponents, while the second factor is computed in the future and they become independent for $n \to \infty$ (in the special case of the generalized baker transformation, they are independent for any n).

In spite of this subtlety, the local approach is conceptually simpler than the global one. We should not forget, however, that it is, in general, numerically impossible to measure spectra of pointwise quantities directly. The only way to use relations (3.23) and (3.26) numerically seems, in general, via the global approach outlined in the previous subsections.

The problem that for nonperiodic points one encounters difficulties that are absent for periodic points is rather uncommon and seems to be related to the fact that we are interested in properties of point sets of measure zero. Sets of nonzero measure on strange attractors seem to be well characterized by the periodic orbits nearby, in general. That this need not be the case, if one studies the questions treated in this paper, will be found again in Section 4.

Finally, we show the relations between the spectrum $f(\alpha_2)$ of crowding indices and that of Liapunov exponents $\phi(\Lambda)$. For this purpose, we must express both distributions in terms of the same scaling parameter. This can be done by referring to constant-mass coverings, already introduced in Section 2 for crowding indices [see Eq. (2.16)]. We can now do the same for effective Liapunov exponents. Consider again map (3.27): since $\exp(-n\lambda_1)$ represents the mass in the horizontal strip, we fix it equal to some value p and determine a variable number of iterations $n(\mathrm{x})$ such that $p = \exp[-n(\mathrm{x})\,\lambda_1(\mathrm{x}, -n(\mathrm{x}))]$. The associated distribution of λ_1, λ_2 is of the form [see Eq. (3.7)]

$$P(\Lambda, p) = |\ln p|^{1/2}\, p^{\phi(\Lambda)/\Lambda_1} \tag{3.30}$$

Under these assumptions, we can conjecture that the probability to find a crowding index $\alpha_2 = -\Lambda_1/\Lambda_2$ is [see Eqs. (3.29) and (2.16)]

$$|\ln p|^{1/2}\, p^{1-f(\alpha_2)/\alpha_2} = |\ln p|^{1/2} \int p^{\phi(\Lambda_1, -\Lambda_1/\alpha_2)/\Lambda_1}\, d\Lambda_1 \tag{3.31}$$

In the next subsection, we compare this local approach with the global one of the previous subsection, showing with some simple examples that they are in agreement.

3.4. Special Two-Dimensional Maps

For all hyperbolic attractors in one and two dimensions, Eqs. (3.13) and (3.14) simplify to

$$\tau_0(q) = -g^{(1)}(1-q), \qquad \alpha_0(q) = \left.\frac{dg^{(1)}(z)}{dz}\right|_{z=1-q} \tag{3.32}$$

where $g^{(1)}(z)$ is the generating function for the first (positive) effective Liapunov exponent. We have already considered here that $D_1(q) = 1$ and thus that $\alpha_1 = 1$ and $\tau_1 = q - 1$. For the spctra of α_0 and Λ_1, this implies

$$f_0(\alpha_0) = \alpha_0 - \phi^{(1)}(\alpha_0) \tag{3.33}$$

This equation holds, indeed, also for one-dimensional maps. Further simplifications arise if one has more structure:

(i) Generalized baker transformations of the type

$$\begin{aligned} y' &= 2y \bmod 1 \\ x' &= F_{[2y]}(x) \end{aligned} \tag{3.34}$$

where $[z]$ is the integer part of z, and F_0 and F_1 are two functions mapping the interval $[0, 1]$ into two disjoint subintervals $J_i \in [0, 1]$. In this case, one has $\lambda_1 = \ln 2$. Also, all cross-correlations between λ_1 and λ_2 are absent, leading to

$$g(z_1, z_2) = z_1 \ln 2 + g^{(2)}(z_2) \tag{3.35}$$

As a consequence, Eqs. (3.20) and (3.14) can be combined to

$$-\Lambda_2(-\tau(q))\,\alpha_2(q) = \ln 2 \tag{3.36}$$

This is a result for the projection of the invariant measure onto the non-trivial axis. This projection is also the maximum entropy measure of the repeller $x' = F_i^{-1}(x)$ for $x \in J_i$. In the latter context, Eq. (3.36) was first derived in Ref. 23. Equation (3.36) is a particular case of Eq. (3.29), with $\lambda_1 = \ln 2$.

(ii) Maps with constant Jacobian: writing the Jacobian as $|J| = \exp(-B)$, we have

$$P(\Lambda; n) = \delta(\Lambda_1 + \Lambda_2 + B)\, P^{(1)}(\Lambda_1; n) \tag{3.37}$$

where $P^{(1)}(\Lambda_1; n)$ is the distribution of the first effective Liapunov exponent. As a consequence, we obtain

$$g(z_1, z_2) = g^{(1)}(z_1 - z_2) - Bz_2 \tag{3.38}$$

Equations (3.19) and (3.20) become, then

$$g^{(1)}(\tau_2(q)-q+1)=-B\tau_2(q) \tag{3.39}$$

and

$$\alpha_2(q)=\frac{\Lambda_1^*(q)}{\Lambda_1^*(q)+B}, \qquad \Lambda_1^*(q)=\left.\frac{dg^{(1)}(z)}{dz}\right|_{z=\tau_2(q)-q+1} \tag{3.40}$$

After some manipulations, this leads finally to[39]

$$\alpha_0 f_2(\alpha_2)=\alpha_2 f_0(\alpha_0), \qquad \alpha_2=\alpha_0/(\alpha_0+B) \tag{3.41}$$

For actual computations of dimension, Eq. (3.41) seems to be most useful. Equations (3.40) and (3.41) are again in full agreement with the results of the previous section. In fact, from Eq. (3.29), recalling that $\lambda_2=-B-\lambda_1$, we recover the first of (3.40), once α_2 and λ_1 are interpreted as the local crowding index and the effective Liapunov exponent corresponding to the same box, as described above.

Equation (3.41) can also be derived in a straightforward way from Eq. (3.31). In fact, in the case of two-dimensional maps with constant Jacobian, there is only one pair λ_1, λ_2 that yields a preassigned α_2. The occurrence frequency of α_2 is therefore equal to the frequency of λ_1, provided that α_2 and λ_1 are related by Eq. (3.40). Equation (3.41) is, then, a consequence of (3.31) and (3.40).

(iii) Generalized baker transformations of the form (3.27). Following the local approach, it is clear that Eq. (3.41) holds for all two-dimensional maps in which there is a one-to-one correspondence between the positive and the negative Liapunov exponents. The map defined in Eq. (3.27) belongs to this class. In fact, λ_1 is, in general, given by

$$e^{n\lambda_1}=p_1^{-i}p_2^{-(n-i)} \tag{3.42}$$

where i is the number of times the first multiplier $1/p_1$ occurred in n iterations:

$$i=\frac{\lambda_1+\ln p_2}{\ln(p_2/p_1)}n \tag{3.43}$$

The second Liapunov exponent is determined by

$$e^{n\lambda_2}=r_1^i r_2^{n-i} \tag{3.44}$$

By eliminating i between (3.43) and (3.44), we can express λ_2 as a function of λ_1:

$$\lambda_2 = \frac{\ln(r_1/r_2)}{\ln(p_2/p_1)}(\lambda_1 + \ln p_2) + \ln r_2 \tag{3.45}$$

Accordingly, by using Eq. (3.45) in place of the first of Eqs. (3.40), we find that Eq. (3.41) also holds for the generalized baker transformation, a result which also follows from Eq. (3.31).

(iv) Conformal maps: here, one has $\lambda_1(z) = \lambda_2(z)$, $z = x + iy$. Thus, if the map is chaotic, one does not have an attractor, but a repeller. In the case of a rational map $z' = \mathsf{F}(z)$, the repeller is called a Julia set.[40] The most interesting invariant measure is the balanced invariant measure,[40] obtained by iterating backward with equal probability for all roots of F^{-1}. This measure can be related to the natural measure on the attractor by the folowing simple trick: in addition to the two variables $x = \Re(z)$ and $y = \Im(z)$, include a third variable $w \in [0, 1]$. If F^{-1} has p roots, denoted by $\{\mathsf{F}_0^{-1}, \ldots, \mathsf{F}_{p-1}^{-1}\}$, consider the three-dimensional map

$$(w, z)' = (pw \bmod p, \mathsf{F}_{[pw]}^{-1}(z)) \tag{3.46}$$

where $[x]$ denotes the integer part of x. It is clear that the natural measure of this map is uniform in the w direction and that its projection onto the z plane gives exactly the balanced invariant measure.

System (3.46) has one positive Liapunov exponent $\lambda_1 = \ln p$ and two negative ones of equal magnitude $-\lambda(z)$. The generating function for Eq. (3.46) can then be written as

$$g(z_1, z_2, z_3) = z_1 \ln p + g^{(J)}(-(z_2 + z_3)) \tag{3.47}$$

where $g^{(J)}(z)$ is the generating function for the Liapunov exponent λ of the original Julia set. We denote by D its dimension [*not* that of the attactor of Eq. (3.46)] and use $\tau = (q-1)D$. Equations (3.13) and (3.14) are now trivial [$K(q) = \ln p$], and Eqs. (3.19) and (3.20) become

$$g^{(J)}(\tau(q)) = (q-1)\ln p \tag{3.48}$$

and

$$\Lambda(-\tau(q))\,\alpha(q) = \ln p \tag{3.49}$$

For $q = 0$ and $q = 1$, Eq. (3.48) agrees with rigorous results obtained in Ref. 41.

4. THE LOGISTIC MAP

The main problem with the formalism developed in the last two sections is that it is not clear how far it can be extended to nonhyperbolic systems. In order to find its limitations, we thus study the simplest nonhyperbolic system, before treating the more interesting Hénon map, in the next section.

4.1. Fully Developed Chaos

The simplest case is that of "fully developed" chaos, i.e.,

$$x' = F(x) = 1 - 2x^2 \tag{4.1}$$

In this case, everything can be computed exactly by using the conjugacy to the "roof" map[42]

$$y' = 1 - 2|y| \qquad \text{for} \quad x = \sin\frac{\pi y}{2} \tag{4.2}$$

The natural measure has the density

$$\frac{d\mu(x)}{dx} = \frac{1}{\pi(1-x^2)^{1/2}} \tag{4.3}$$

For didactic purposes, the generalized dimensions of this density are computed by box counting, with box size ε, without using Eq. (4.2), which would yield the same result. The weights of the first and last boxes (those at $x = \pm 1$) are propositional to $\sqrt{\varepsilon}$, while the weights of all other boxes are roughly proportional to ε. Thus, we see that

$$\sum_{i=1}^{1/\varepsilon} p_i^q \sim \varepsilon^{q-1} + \text{const} \cdot \varepsilon^{q/2} \tag{4.4}$$

and, inserting this into Eq. (2.3), we get immediately[16]

$$D(q) = \begin{cases} 1 & \text{if} \quad q \leqslant 2 \\ \dfrac{q}{2(q-1)} & \text{if} \quad q \geqslant 2 \end{cases} \tag{4.5}$$

Hence, $D(q)$ is not unity for all q, in contrast with what we would expect for hyperbolic systems.

Using Eq. (2.12), we obtain the spectrum of crowding indices as

$$f(\alpha)=\begin{cases}2\alpha-1 & \text{for } \frac{1}{2}\leqslant\alpha\leqslant 1\\ -\infty & \text{otherwise}\end{cases} \tag{4.6}$$

Notice that Eq. (2.13) would have only predicted $f(1/2)=0$ $f(1)=1$, without the linear behavior in between. The complete from (4.6) can also be obtained directly from $\hat{P}(\alpha; p)$, using Eq. (4.5) and the third of Eqs. (2.17).

As is clear from the conjugacy to the roof map and from Eq. (2.31), the generalized entropies are $K(q)=\ln 2$ for all q. From Eq. (3.13), we would then expect that the Liapunov spectrum is also trivial: $\phi(\Lambda)=\infty$ for $\Lambda\neq\ln 2$ and $g(z)=z\ln 2$. This is, however, not true. The conjugacy (4.2), in fact, gives

$$e^{G_n(z)}=\int_{-1}^{1} d\mu(x)\,|F^{(n)}(x)'|^z=\frac{1}{2}2^{nz}\int_{-1}^{1} dy\left|\frac{\cos(\pi y_n/2)}{\cos(\pi y/2)}\right|^z \tag{4.7}$$

where y_n is the nth iterate of y. For $-1<z\leqslant 1$, the zeros of the cosines have no influence on the asymptotic behavior: hence, $g(z)=G_n(z)/n=\ln 2$. For $z>1$, the zeros of the denominator prevail. Since $\cos(\pi y_n/2)\approx 2^n\cos(\pi y/2)$, for $1-|y|\leqslant 2^{-n}$, the integrand is roughly 2^{nz}, for $1-|y|\leqslant 2^{-n}$, and negligible otherwise. This leads to $g(z)=(2z-1)\ln 2$. Finally, consider the zeros of $\cos(\pi y_n/2)$. There are 2^n-1 of them, each with a slope of order 2^n. Together, they imply that the integral diverges at $z=-1$, such that $\exp[G_n(z)]\sim 2^n/(z+1)$ at $z\to -1$. Combining everything, we have

$$g(z)=\begin{cases}\infty & \text{for } z\leqslant -1\\ z\ln 2 & \text{for } -1<z\leqslant 1\\ (2z-1)\ln 2 & \text{for } z\geqslant 1\end{cases} \tag{4.8}$$

and

$$\phi(\Lambda)=\begin{cases}\ln 2-\Lambda & \text{for } \Lambda\leqslant\ln 2\\ \Lambda-\ln 2 & \text{for } \ln 2\leqslant\Lambda\leqslant\ln 4\\ \infty & \text{for } \Lambda\geqslant\ln 4\end{cases} \tag{4.9}$$

The nontrivialities of the Liapunov spectrum are thus due to the unstable fixed point at $x=-1$, where the slope is twice as large as in the average, and to the critical point ar $x=0$. Equation (4.9) implies that the scaling function $f_0(\Lambda)=\Lambda-\phi(\Lambda)$ displays a straight-line behavior with slope 2 for $\Lambda\leqslant\ln 2$, is constant (equal to $\ln 2$) for $\ln 2\leqslant\Lambda\leqslant\ln 4$, and is $-\infty$ for

$\Lambda > \ln 4$. Indeed, effective Liapunov exponents assume all values between $-\infty$ and $\ln 4$.

We should point out that a different result would have been obtained if we had based the definition of effective Liapunov exponents on periodic orbits, with the generating function $G(n, z)$ being an average over all orbits of period n. In that case, we would find the same value $\lambda = \ln 2$ for all orbits, except for the fixed point $x = -1$, where $\lambda = \ln 4$. In particular, the spectrum of Liapunov exponents of periodic points cannot extend to negative values (as it does for nonperiodic points), as this would mean that we have attracting periodic orbits and no chaotic attractor.

Since the pointwise dimension is $\alpha(x) = \frac{1}{2}$ at $x = \pm 1$, we see that Eq. (3.23), written now as $\alpha_0(x) = \alpha(x)\,\lambda(x)$, is indeed satisfied in all periodic points with $\alpha_0(x) = 1$, including at $x = \pm 1$. There, the anomaly in λ is exactly compensated by an anomaly in α. But Eq. (3.23) does not hold at *all* points, including nonperiodic ones: for $x = 0$ and all its preimages, our ansatz (3.22), from which (3.23) was deduced, is simply wrong. Instead of Eq. (3.22), one has in these points different asymptotic behaviors in the two limits $n \gg |\ln \varepsilon| \to$ and $|\ln \varepsilon| \gg n \to \infty$:

$$p(\varepsilon, n, x = 0) \approx \begin{cases} 2^{1-n}\sqrt{\varepsilon} & \text{for} \quad n > \ln \varepsilon / \ln 4 \\ 2\varepsilon & \text{for} \quad n < \ln \varepsilon / \ln 4 \end{cases} \tag{4.10}$$

Accordingly, pointwise entropies cannot be defined via Eq. (3.22) at $x = 0$ and at all its preimages. We should not be surprised, then, that these points create problems in the global approach if they make any contribution there. As we have seen, they indeed do contribute at sufficiently large q ($q > 2$ in the present case) and sufficiently small α ($\alpha < 1$). Intuitively, the problem with these points is that due to the folding, the map cannot be linearized there and our simple arguments of Section 3 break down. Expressed more technically, the bounded variation principle of Ref. 23 breaks down in these points, and the action of the map in any small but finite neighborhood is not characterized by the Liapunov exponents at these points.

Instead of using Eq. (3.22), effective Liapunov exponents and pointwise dimensions could also have been defined via generating partitions. Call Γ the generating partition into $x > 0$ and $x < 0$, and $\Gamma^{(n)}$ its nth preimage. Each interval of $\Gamma^{(n)}$ defines one cylinder set of length n. The integrals of the natural measure μ over such intervals decrease in the (geometric) average as $\exp[-nK(1)]$, while their lengths decrease as $\exp(-n\lambda)$. For any point $x \neq 0$ that is not a preimage of $x = 0$, we can define $\alpha_0(x)$ by $\mu_x^{(n)} \approx \exp[-n\alpha_0(x)]$, where $\mu_x^{(n)}$ is the mass of the interval in $\Gamma^{(n)}$ containing x, and define $\lambda(n, x)$ analogously via the length of these

intervals. For $x=0$ and for its preimages, we can take the largest of the two intervals next to them. We see easily that this gives $\alpha_0(x)=\ln 2$ at *all* points. For the Liapunov exponents it gives $\lambda=\ln 4$ at $x=\pm 1$, and $\lambda=\ln 2$ for all other points, including $x=0$. Equation (3.23) holds then indeed for *all* points. The Liapunov spectrum $\phi(\Lambda)$, defined via sums over all interval sin $\Gamma^{(n)}$, consists then only of the linear piece between $\Lambda=\ln 2$ and $\Lambda=\ln 4$, without the linear piece at $\Lambda<\ln 2$ in Eq. (4.9).

The last argument, based on a generating partition, thus leads to the simplest results in the case of fully developed chaos in one-dimensional maps. Its drawback is that it is not so easy to apply numerically to other one-dimensional maps, such as those discussed below, and even more so in higher dimensional systems, such as the Hénon map.

4.2. "Typical" Chaos

It is thus interesting to see whether such problems appear when the critical point is *not* mapped onto any periodic orbit, after any finite number of iterations. We call this "typical" chaos, since it appears on a set of control parameter values of nonzero measure. We shall now show that also

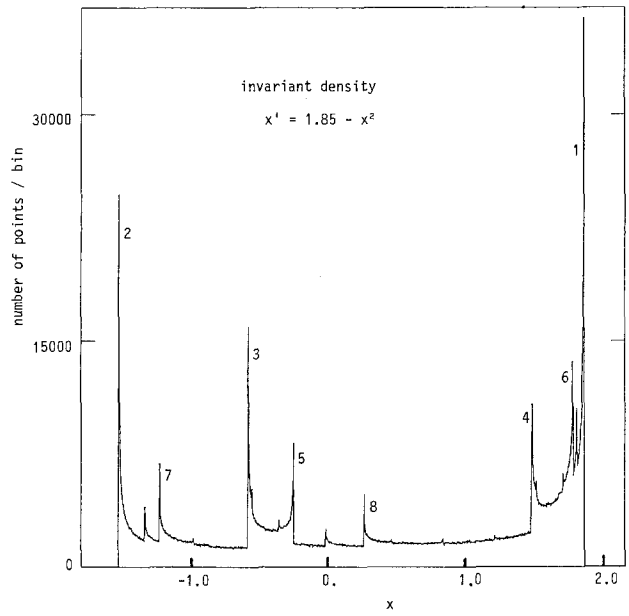

Fig. 1. Density of the natural measure of the map $x_{n+1}=1-1.85x_n^2$. Notice the spikes at the forward images of the critical point $x=0$. The kth image is labeled by k.

in this case the formalism of Sections 2 and 3 does not hold without modifications.

First, we see that the density of the natural measure has square-root singularities at all forward images of the critical point, as shown in Fig. 1. These singularities, being denumerable, should have exactly the same effect on the generalized dimensions and on the spectrum of crowding indices as the same singularity had in the fully developed case. We thus expect Eqs. (4.5) and (4.6) to hold again.

As a numerical test of the latter, we show in Fig. 2 the box-counting distribution $\tilde{P}(\alpha;\varepsilon)$ for $a=1.85$ and 5×10^5 nonempty boxes on a log-log plot, rescaled in such a way that the curve should approach $f(\alpha)$ versus α for $\varepsilon\to0$, according to Eq. (2.17). The support of μ has been renormalized

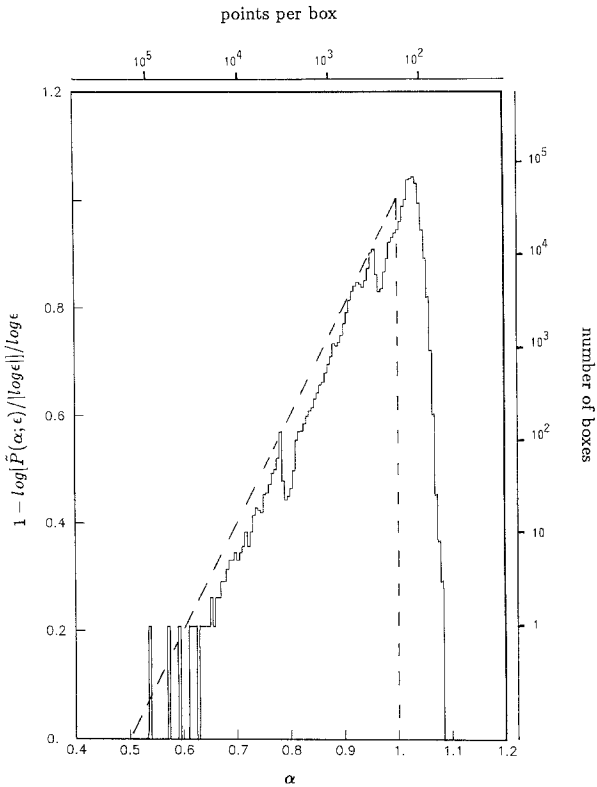

Fig. 2. Histogram of the distribution of the number of boxes with a given weight for the logistic map at $a=1.85$. The number of nonempty boxes was 5×10^5; the number of iterations was 10^8. The data are displayed on a log–log plot with scales chosen in such a way that the horizontal axis is α and the vertical would be $f(\alpha)$ in the limit $\varepsilon\to0$. The dashed line represents Eq. (4.6).

to 1, with a proper choice of the unit length. For comparison, the conjectured $f(\alpha)$ is also shown in Fig. 2. We find indeed reasonable agreement. The function $D(q)$, as obtained from this by Legendre transform, is shown in Fig. 3 (dashed line). Also shown there is the direct estimate of $D(q)$ via Eq. (2.3) (solid line). We see that they agree very poorly. This should not be too surprising, since the moments $\langle p(\varepsilon)^{q-1} \rangle$ are analytic in q and a singularity as in Eq. (4.5) can only develop in the limit $\varepsilon \to 0$. This is very similar to a phase transition in statistical mechanics, which only appears in the thermodynamic limit. It should be a warning against computing $f(\alpha)$ by first evaluating the moments and then by performing a backward Legendre transform.[3] While this can speed up convergence, it might have led some authors to overlook possible phase transition-like behavior in nonuniform fractals, such as those occurring in connection with a Joule energy distribution on conducting percolating clusters.[43] We might add that such phase transitions do exist for Joule energy distributions on conductors in the form of some Sierpinski-type lattices[44] and for the Cantor set of irrational winding numbers in critical circle maps.[45]

We should comment on the dashed curve in Fig. 3, obtained by Legendre-transforming the data of Fig. 2. Its poor agreement with the exact result (dotted line) can easily be understood and, accordingly, might have been corrected: in fact, in plotting Fig. 2, we have taken the entire support

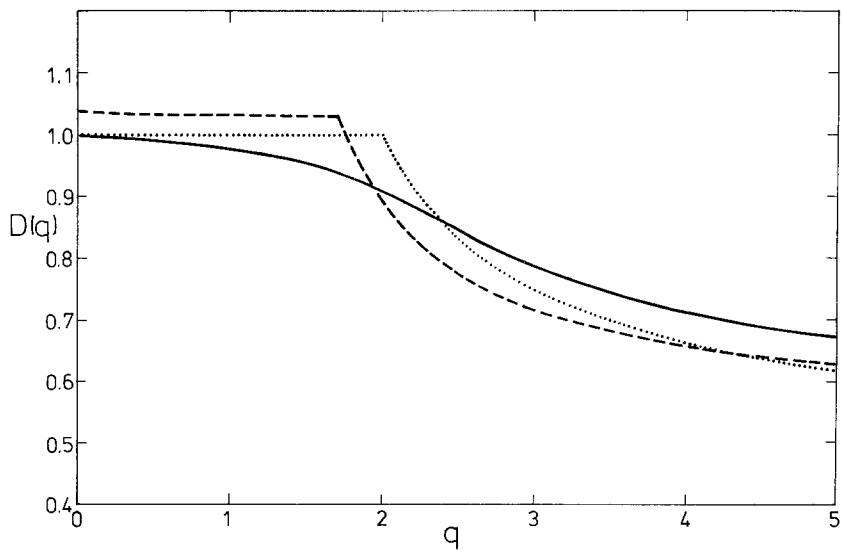

Fig. 3. The dimension function $D(q)$ from the data shown in Fig. 2. (···) Exact result. (– –) Legendre transform of the curve in Fig. 2 [in the version of Eq. (2.12), divided by $q-1$]. (—) from Eq. (2.3), but with $\varepsilon = 2 \times 10^{-6}$, instead of taking the limit $\varepsilon \to 0$.

$[a-a^2, a]$ of the masure as our unit length (we iterated the map $x' = a - x^2$). If we take, instead, the length unit as an open parameter, we can shift both axes by essentially the same arbitrary amount. In particular, we can shift them such that the maximum is at $\alpha = 1$, in which case we also find $f(\alpha = 1) = 1$ and $\alpha_{\min} = 1/2$. This improves considerably the agreement in Fig. 3.

Perfect agreement is achieved if we take into account that the bin at $\alpha_{\min}$ contains a single nonempty box, whence asymptotically $f(\alpha_{\min})$ should be shifted down from 0.2 to zero. Without discussing these corrections again in detail, we apply them in the next subsection when we deal with the Hénon map.

We next study the Liapunov spectrum. Numerical results, again for $a = 1.85$, are shown in Fig. 4. More precisely, we plot the quantity $-(1/n)\ln[P(\Lambda; n)/\sqrt{n}]$, for $n = 20$, 40, and 60, obtained from 6×10^8 iterations. According to Eq. (3.7), the curves in Fig. 4 should tend to $\phi(\Lambda)$ for $n \to \infty$. Indeed, we see rather slow convergence.

As in the case of fully developed chaos, the spectrum of Fig. 4 is not confined to positive Λ. Of course, there cannot be any periodic orbits with

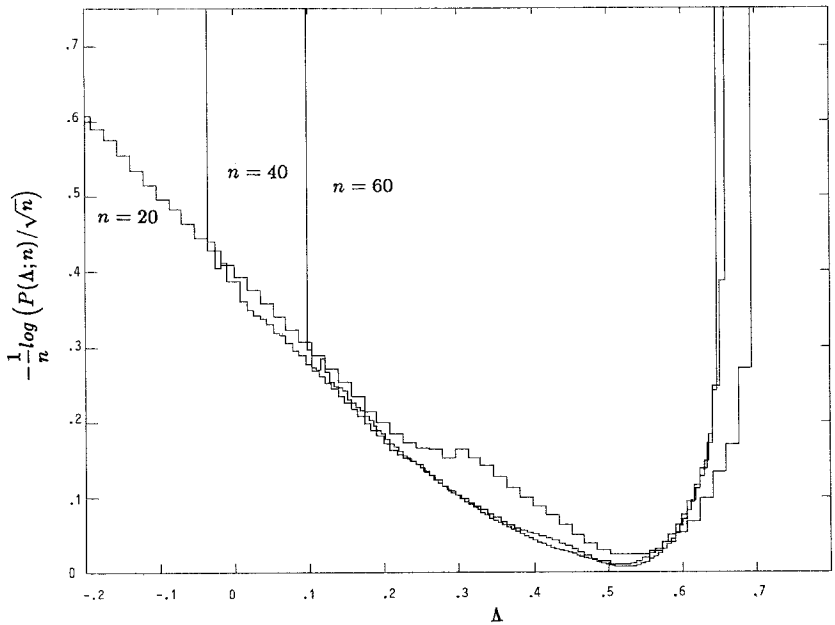

Fig. 4. Probability densities $P(\Lambda; n)$ of efective Liapunov exponents Λ for the logistic map with $a = 1.85$ and with $n = 20$, 40, and 60. The number of iterations was 6×10^8. The logarithmic scale is chosen such that the curves should become plots of $\phi(\Lambda)$ versus Λ for $n \to \infty$.

a negative Λ, since they would be attractors.[4] The problem is that a strange attractor is the closure of all periodic orbits that, in hyperbolic systems, fill densely the support of the Liapunov spectrum. Naively, one might have expected the same in the present case, but we see again that we must be more careful. On the other hand, the tail in the Liapunov spectrum for small Λ, as observed in Fig. 4, can easily be explained heuristically. Let us consider sequences of N iterates that give an effective Liapunov exponent Λ smaller than or equal to zero. Such a Λ can only arise if one of the N iterates is close to the maximum. Therefore, we need to evaluate the mass contained in an interval of size ε such that an initial condition belonging to it will yield an effective Liapunov exponent (over N iterates) smaller than Λ. Assuming that the initial n iterates fall "far" from the maximum (i.e., on generic points), they will yield a multiplier $e^{n\langle\lambda\rangle}$, with $\langle\lambda\rangle$ being the average Liapunov exponent. The $(n+1)$th multiplier will be of the order of the distance from the maximum: that is, of the order of the length $\varepsilon e^{n\langle\lambda\rangle}$ of the interval, after the first n iterates. Finally, the contribution of the remaining $N-n-1$ iterates will be $e^{(N-n-1)\langle\lambda\rangle}$. Imposing that the total multiplier, given by the product of these three terms, be equal to $e^{N\Lambda}$, we determine ε as

$$\varepsilon \sim \text{const} \cdot e^{N\langle\lambda\rangle} \tag{4.11}$$

giving $\phi(\Lambda) \sim \text{const} - \Lambda$. The constant can be estimated from Eq. (3.32) with $q=2$ and from Eq. (3.8). They give, respectively, $g^{(1)}(-1) = -K(2)$ and [using $\phi(0)' = -1$]

$$g^{(1)}(-1) = -\phi(0) \tag{4.12}$$

Furthermore, we expect the linear behavior of $\phi(\Lambda)$ to hold not only for $\Lambda \to -\infty$, but for all $\lambda < \lambda_c$, where λ_c is defined as the largest value of Λ at which the slope of $\phi(\Lambda)$ is -1. Taking all this together, we find

$$\phi(\Lambda) = K(2) - \Lambda \qquad \text{for} \quad \Lambda \leqslant \lambda_c \tag{4.13}$$

where the presence of $K(2)$ is due to the coincidence of the spectra of metric entropies and effective Liapunov exponents, for $\Lambda > \lambda_c$. It is also useful to consider the value $\Lambda = \lambda_{\min}$ where the spectrum $\Lambda - \phi(\Lambda)$ is equal

[4] We monitored, during the iteration, against being on a periodic orbit by running simultaneously to the trajectory $\{x_n\}$ another trajectory $\{y_n\}$ with $x_0 = y_0$, but with $y_{n+1} = F^{(2)}(y_n)$. While x_n performs one cycle, y_n performs two, and thus must overtake x_n once. Hence, one only has to monitor that never $y_n = x_n$, for $n \geqslant 1$, in order to be sure not to be on a cycle.[46]

to zero (for example, in Fig. 5, $\lambda_{\min} \approx 0.2$). Since the spectrum $f_0(\alpha_0)$ of metric entropies is nonnegative, we expect it to differ from $\Lambda - \phi(\Lambda)$ for $\Lambda < \lambda_{\min}$. The problem of the possible coincidence of the two spectra in the intermediate region $\lambda_{\min} \leqslant \Lambda \leqslant \lambda_c$ remains open. In addition, further information comes from the spectrum of Liapunov exponents of periodic orbits, which stops at $\lambda = \lambda^p_{\min}$, where $\lambda^p_{\min}$ is the smallest Liapunov exponent of a periodic trajectory. In the case investigated numerically ($a = 1.85$), among all orbits with period $\leqslant 33$, we found $\lambda^p_{\min} \approx 0.237$ (this value belonging to a period-11 orbit). Clearly, we must have $\lambda_{\min} \leqslant \lambda^p_{\min} \leqslant \lambda_c$. Whenever these three quantities coincide, the positive parts of three spectra (metric entropies, effective Liapunov exponents, and periodic orbits) also coincide.

With regard to the distribution of metric entropies, we note that the kneading sequence does not yield the heaviest contribution, in contrast

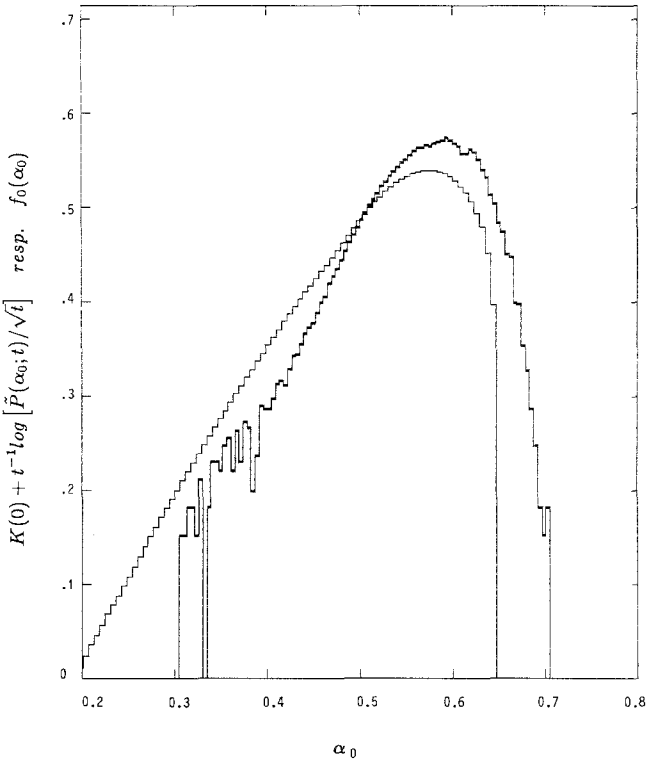

Fig. 5. Heavy lines: histogram of weights of symbol sequences for the logistic map with $a = 1.85$. The length of the symbol sequences is $t = 23$. The number of iterations was 1.2×10^7. The logarithmic scale is chosen in such a way as to give the spectrum of temporal crowding indices $f_0(\alpha_0)$ for $t \to \infty$. Light lines: function $f_0(\Lambda) \equiv \Lambda - \phi(\Lambda)$, with $\phi(\Lambda)$ approximated by the $n = 60$ data of Fig. 4.

with what one might have guessed. In fact, assuming again that the orbit of forward images of the critical point be "typical," the weight of the kneading sequence over N iterates is readily computed. All trajectories whose foward symbol sequence (of length N) coincides with the kneading sequence start from points lying in an interval of width

$$\varepsilon^{-N\langle\lambda\rangle/2} \tag{4.14}$$

around $x=0$ at time $n=0$. Since the invariant measure is nonzero and smooth around the critical point, we conclude that the mass of the kneading sequence decreases according to Eq. (4.14). With the Liapunov exponent of the period-11 cycle smaller than $\langle\lambda\rangle/2$, the symbol sequence of this cycle becomes heavier than the kneading sequence for N sufficiently large. This has been verified numerically, noting that, for $N>20$, one finds increasingly more sequences that have a larger weight than the (beginning of the) kneading sequence.

By comparing the spectrum of pointwise entropies $f_0(\alpha_0)$ with that of effective Liapunov exponents, we see that they are in satisfactory agreement for $\Lambda>0.3$. A qualitatively similar behavior has been found for the spectrum of Liapunov exponents from periodic orbits. We might add that the maximal λ (equal also to the maximal pointwise entropy) is $\lambda_{\max}$ and corresponds to the fixed point $x=0.513$.

5. THE HÉNON MAP

The source of problems with Eq. (1.2) is the presence of homoclinic tangency points, where the map is no longer hyperbolic. The actual occurrence of these tangencies is suggested by Fig. 6, where the attractor, which coincides with the unstable manifold of the fixed point

$$x^*=y^*=\{b-1+[(b-1)^2+4a]^{1/2}\}/(2a)$$

is shown together with part of the stable manifold of that fixed point. The blowup shown in Fig. 7 suggests that if we followed the stable manifold further, the two manifolds would come closer and closer to touching each other. If there are any homoclinic tangencies, it is obvious that there must be a dense set of them, if the atractor is indeed ergodic. Since such tangency points are in many ways similar to the critical point $x=0$ of the logistic equation (1.1), we expect that the Hénon map behaves essentially as the latter, with only minor modifications due to its two-dimensionality.

5.1. Liapunov Spectra

Since the Hénon map has a constant Jacobian, we have only one independent Liapunov exponent and the discussion of Section 3.4(ii)

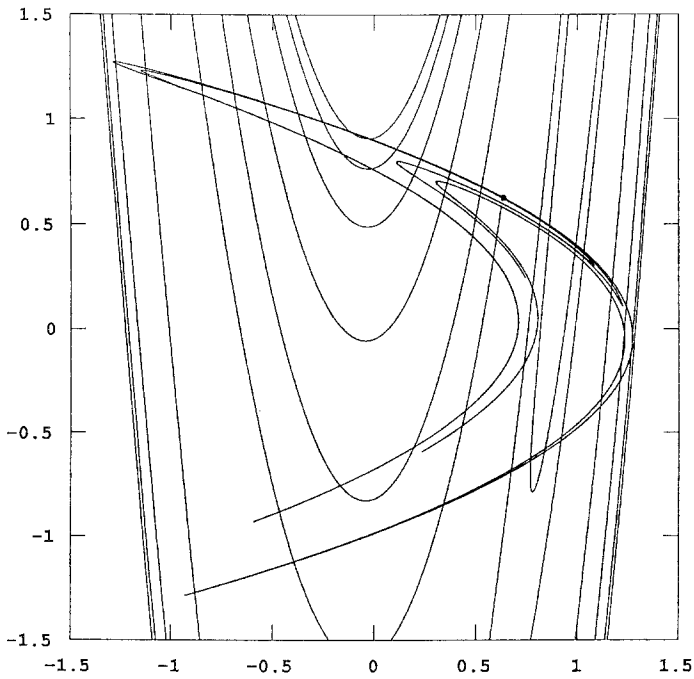

Fig. 6. The Hénon attractor with parameters $a = 1.4$ and $b = 0.3$, together with part of the stable manifold of the manifold of the fixed point (x^*, y^*). The unstable manifold coincides with the attractor.

applies. The distributions $P^{(1)}(\Lambda_1; n)$ with $n = 12$ and 24 are shown in Fig. 8. Again, the presentation is such that the curves should converge to $\phi^{(1)}(\Lambda_1)$ versus Λ_1 for $n \to \infty$. Figure 8 indicates a faster convergence than in the logistic map. This is not surprising: in fact, any quantity such as an effective Liapunov exponent is an average over all leaves in the Cantor set of Fig. 6. Hence, deviations from scaling arising on a single leaf are smeared out. Second, we see that also in the present case the leading Liapunov exponent can be negative for any finite n. This creates the same problem as in the one-dimensional case, namely that the spectrum cannot agree with the spectrum of Liapunov exponents of *periodic* orbits. At the same time, however, we can apply essentially the same argument as in the last section in order to estimate $\phi^{(1)}(\Lambda_1)$ for $\Lambda_1 \leqslant 0$.

We first observe that there is no indication in Fig. 7 that homoclinic tangencies are avoided. Second, Fig. 7 suggests that further magnification would show that, near the forward images of the "prominent" homoclinic tangency points (HTPs) the stable manifold approaches a set of straight

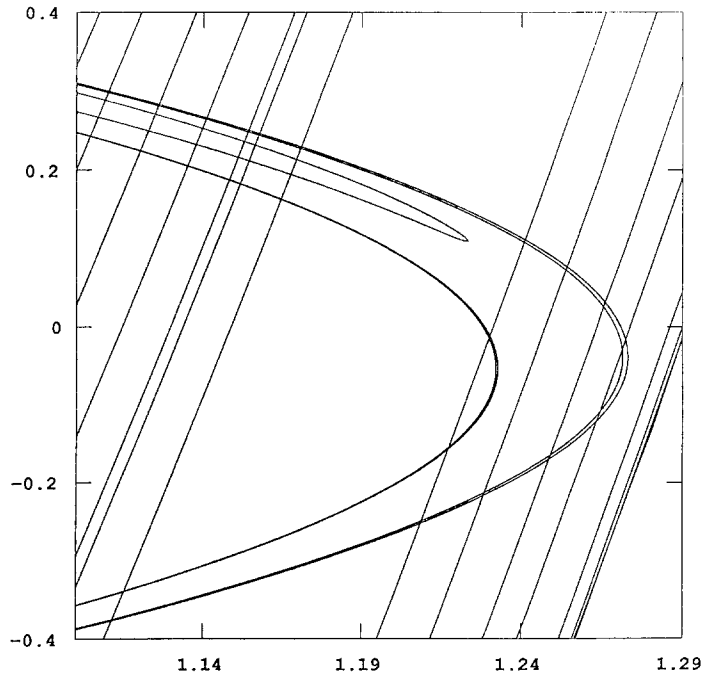

Fig. 7. Enlarged part of Fig. 6, with the stable manifold extended further. There does not seem to be any tendency that homoclinic tangencies are avoided by any unknown mechanism.

lines, while the unstable manifold can be approximated by a Cantor set of parabolas. More precisely, assume that $P=(x, y)$ is a HTP. Then its image $F(P)$ and its preimage $F^{-1}(P)$ are also HTPs. In the limit $n \to \infty$, the radius of curvature $R_u^{(n)}$ of the unstable manifold at $F^n(P)$ tends to zero, while the radius $R_s^{(-n)}$ of the stable manifold tends to zero at $F^{-n}(P)$. The "prominent" HTP P_0 is the one where $1/R_u^{(n)} + 1/R_s^{(n)}$ is minimal. The above approximation by parabolas and straight lines should hold in the neighborhood of $F^n(P_0)$ for large n, after a suitable n-dependent linear rescaling. A simple "model" of what happens near a forward image of a prominent HTP is thus the following: we replace the unstable manifold with a Cantor set of parabolas and the stable manifold with a dense set of parallel straight lines. The action of the map in this neighborhood is approximated by a linear transformation with contraction by a fixed factor γ along the stable manifold and expansion by a factor $\beta = |b|/\gamma$ transverse to it (see Fig. 9). The invariant measure is assumed to be smooth along all branches of the unstable manifold. Finally, small values of Λ_1 are assumed to arise *only* from trajectories that pass near one of the tangency points.

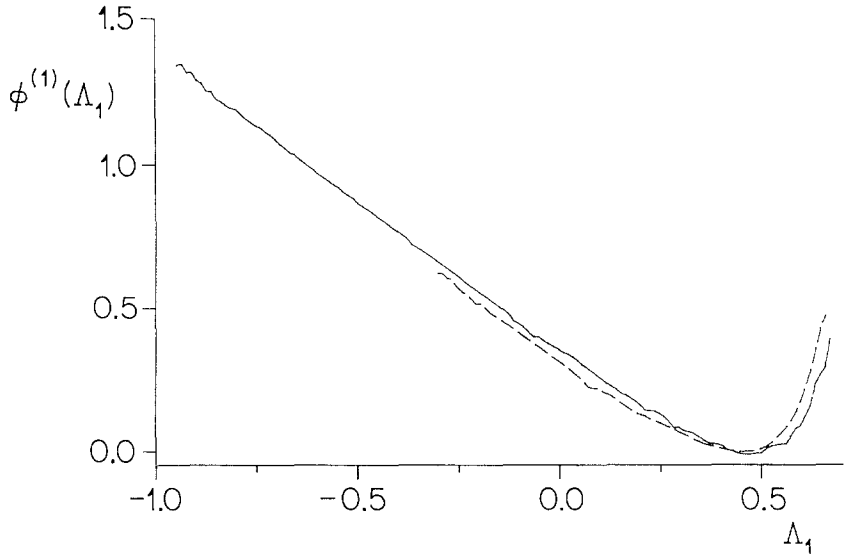

Fig. 8. Spectrum of the first effective Liapunov exponent of the Hénon map with $a = 1.4$, $b = 0.3$, computed from 4×10^9 iterations. The plot is such that again we obtain the scaling function $\phi^{(1)}(\Lambda_1)$ versus Λ_1 in the limit $n \to \infty$. The two curves correspond to (—) $n = 12$ and (– –) $n = 24$.

These assumptions allow us immediately to compute the tail of the Liapunov spectrum. By the same arguments as in the logistic map, we find a linear behavior with slope 1,

$$\phi^{(1)}(\Lambda_1) = K(2) - \Lambda_1 \qquad \text{for} \quad \Lambda_1 < \lambda_{1,\min} \tag{5.1}$$

except that now this cannot be extended down to $\Lambda_1 = -\infty$. Instead, the curve has to be cut off at $\Lambda_1 = \frac{1}{2} \ln |b|$.

Figure 8 is fully compatible with this prediction and suggests that our model is basically correct. In the next subsection, we discuss its implications for the dimension scaling function.

5.2. Dimensions and Spatial Crowding

In order to obtain the fractal dimension directly (without using the Liapunov spectrum), we first follow a box-counting procedure. In Fig. 10, we show the histogram of the distribution of box weights obtained from coverings with 28672×28672 and 14336×14336 boxes (the number of non-empty boxes were $\sim 9 \times 10^5$ resp. $\sim 4 \times 10^5$). The scales are again such that the curve should tend to $f(\alpha)$ versus α for $\varepsilon \to 0$ and for $\alpha \leqslant \alpha^*$

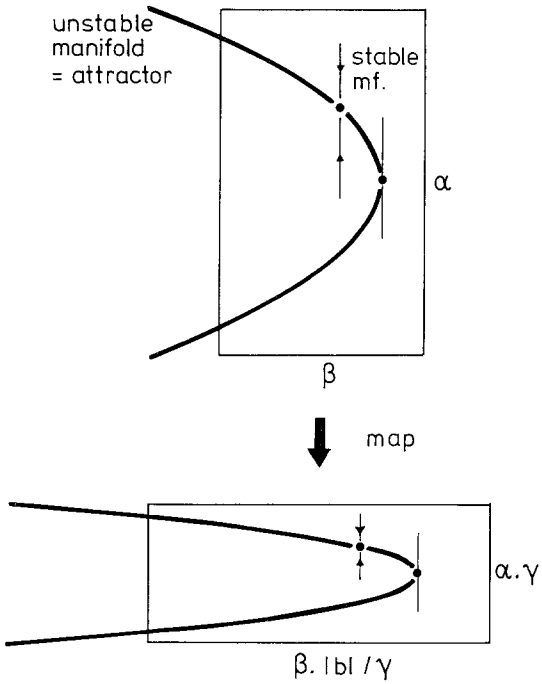

Fig. 9. Simplified "model" of the behavior near hyperbolic tangencies, such as those in Fig. 7. The map is there approximated by a linear transformation.

(corresponding to positive q; for negative q, box-counting has the problems mentioned in Section 2).

The minimal α at which $f(\alpha) \neq 0$ is $\alpha_{\min} = \lim_{q \to \infty} D(q) \leqslant 0.84$. The fact that this value is less than 1 shows that $D_1(q) < 1$ for large q. Since $D_1(q) = 1$ for small q, there must be a singularity at some point $q = q_c$. If the slope of $D(q)$ is discontinuous at this singularity, we must see a linear portion in the curve of $f(\alpha)$ versus α, with slope $f'(\alpha) = q_c$. Indeed, such a behavior can be observed in Fig. 10. The critical value obtained from it is $q_c \approx 2.4$.

Notice that the height of the maximum in Fig. 10 would yield $D(0) \approx 1.3$, in disagreement with values obtained from other methods. This should not bother us too much: the same effect of low convergence was found in Fig. 2 as well. Alternatively, one might estimate $f(\alpha)$ by first evaluating the moments and then by performing a backward Legendre transform, as has been done in other cases.[3,43] This would yield the correct value of $D(0)$, but it would smoothen $D(q)$ and $f(\alpha)$ so strongly that any sign of singularity would be lost. This is exactly the same problem as in the one-dimensional case.

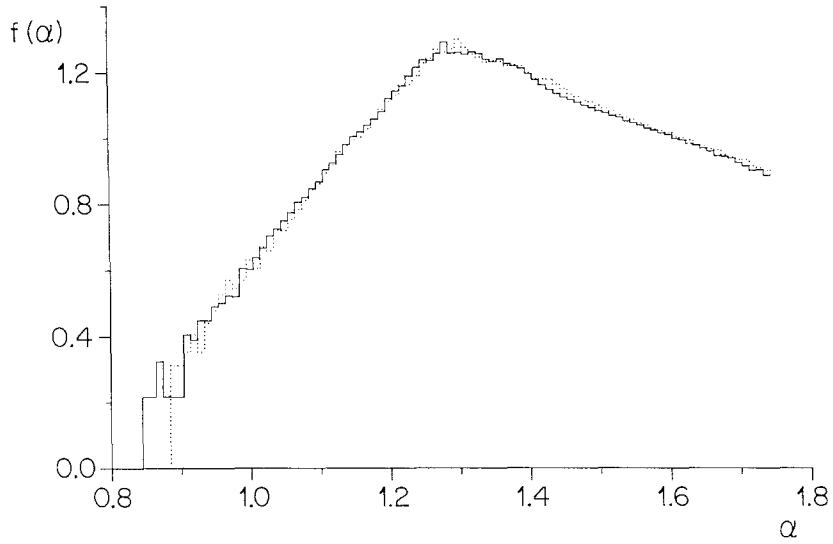

Fig. 10. Histogram of the distribution of the number of boxes with a given weight for the Hénon map with with $a = 1.4$ and $b = 0.3$. The number of nonempty boxes was $\approx 9 \times 10^5$ and the number of iterations was 4×10^9. (—) Grid containing 28762×28762 boxes; (···) 14336×14336 boxes. The data are displayed in a log-log plot with scales such that the horizontal axis is α and the vertical would be $f(\alpha)$ in the limit $\varepsilon \to 0$.

As an alternative to box-counting, we tried to estimate $f(\alpha)$ by counting the number of points in randomly located balls with fixed radius, or by measuring the distances of kth nearest neighbors. With both methods, it was impossible to obtain a statistics as good as with box-counting. However, for negative q (where box-counting fails), we found rather strong deviations from scaling from the distribution of kth nearest neighbors. This seems to be a real effect, since this method should work best there (see Section 2), and it agrees with the fact that (somewhat less) strong scaling violations were found also for $q \geqslant 0$.[47,48] These deviations are, however, still smaller than those found in the logistic map (see also below). We conclude that Fig. 10 represents our best direct information on $f(\alpha)$ for $\alpha \leqslant \alpha^*$. In the following, we will confront it with indirect information obtained from Liapunov spectra and with the implications of the simple "model" discussed in the last subsection.

First, we show in Fig. 11 the scaling function $g^{(1)}(z)$, obtained from the $n = 24$ data displayed in Fig. 8, using the Legrendre transform in the version (2.12). The kink at $z = -1$ is a direct consequence of Eq. (5.1).

Next, Fig. 12 shows $D(q)$ obtained from the data in Fig. 11 through Eq. (3.39). Also shown in Fig. 12 are estimates of $D(q)$ from the data of

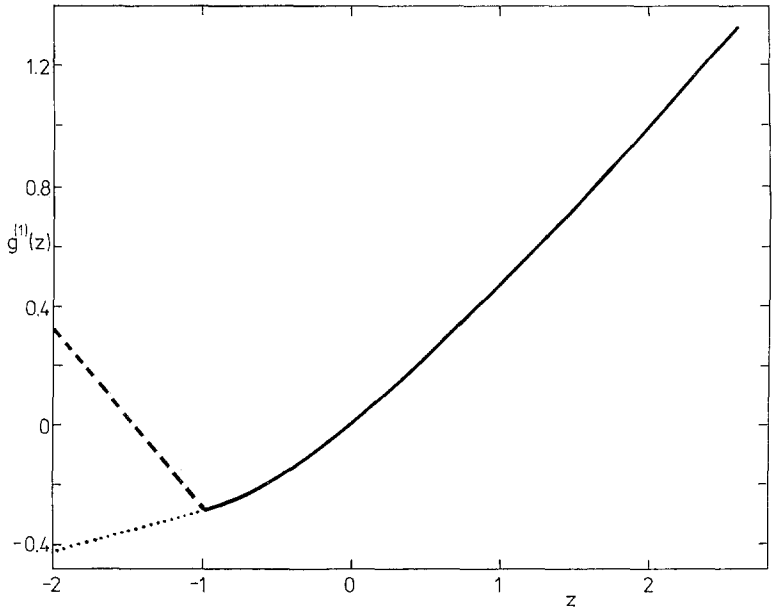

Fig. 11. Scaling function $g^{(1)}(z)$ obtained from the $n=24$ data of Fig. 8 by Legendre transforming, using Eq. (2.12). For $z<-1$, we draw both the result expected from (– –) random orbits and (···) periodic orbits. Neither can be extracted from the data directly. They rely instead on $\Lambda_{1,\min}=\frac{1}{2}\ln b$ and on $\lambda^{p}_{\min}\approx K(2)/2$, respectively.

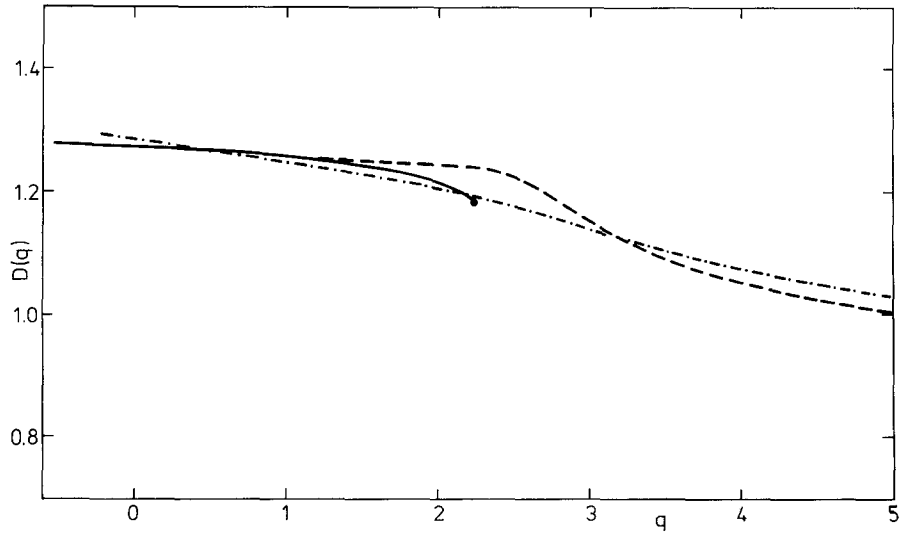

Fig. 12. Dimension function of the Hénon map, obtained from(– –) Fig. 10, via Eq. (2.12), (– –) from the same data using moments, and (—) from Fig. 11, using Eq. (3.39).

Fig. 10, using both the Legendre transform of the $f(\alpha)$ curve (dashed line) and the moments of the probability distribution [Eq. (2.3); dashed-dotted line]. First we notice the quite substantial difference between the latter two curves. This difference is somewhat less dramatic than in the one-dimensional case, but it shown again the danger in extracting dimensions and scaling functions from the moments if these dimensions have singularities.

That there is a singularity in $D(q)$ is most clearly shown by the fact that $D(q=\infty)<1$ from the data of Fig. 10. The latter is also supported by a study of distances of altogether $\sim 10^{11}$ pairs of points in a time series [the actual number of computed distances was much less, as only distances between close pairs ($\varepsilon < 2^{-6}$) were considered]. Due to this, it is clear that we cannot use Eq. (3.39) for arbitrarily large q, as it would give $D(-\infty) \geqslant 1$. We claim that Eq. (3.39) is nevertheless correct for $q \leqslant q_c$ and that q_c corresponds to the argument of $g^{(1)}$ in Eq. (3.39) being -1:

$$z = \tau_2(q_c) - q_c + 1 = -1 \tag{5.2}$$

[It is only below this q_c that the result of Eq. (3.39) is shown in Fig. 12.] Our reason for this conjecture is similar to that in one-dimensional maps: due to the asymptotic behavior (5.1), $g^{(1)}(z)$ is dominated, for $z < -1$, by nonhyperbolic points (homoclinic tangencies), and the arguments of Section 3 are expected to break down there. For $z \geqslant -1$, the "normal" points dominate and we expect Eq. (3.39) to be correct. From Eq. (5.2) we find

$$D_2(q=q_c) = \frac{q_c - 2}{q_c - 1} \tag{5.3}$$

and, from Eq. (3.39) evaluated at q_c, we get $\tau_2(q_c) = K(2)/B$, yielding, finally,

$$q_c = 2 + \frac{K(2)}{|\ln b|} \tag{5.4}$$

Numerically, this gives $q_c \approx 2.24$, in reasonable agreement with the less precise value found from the $f(\alpha)$ spectrum.

It would be interesting to know the Hausdorff dimension of the set of homoclinic tangency points. From what we said above, a positive dimension would mean that the stretch of constant slope in Fig. 10 does not extend down to $\alpha_{\min}$, but ends at some α_- with $f(\alpha_-) > 0$, below which $f(\alpha)$ is again strictly convex. The Hausdorff dimension of the set of homoclinic tangency points with pointwise dimension α would just be $f(\alpha)$, for $\alpha < \alpha_-$. The data shown in Fig. 10 do suggest such a behavior, although they are far from being conclusive in this respect.

6. CONCLUSIONS

We have extended the formalism of the spectra of singularities to multidimensional anisotropic systems, introducing partial pointwise dimensions α_j and partial scaling functions $f_j(\alpha_j)$. We found relations between these, Liapunov exponents, dimensions, and entropies by two complementary approaches: one purely local, involving only pointwise quantities, and one global, involving averages that yield generalized dimensions and entropies. The allowed us to finds links among the various scaling functions $f(\alpha)$, $f_0(\alpha_0)$, $f_j(\alpha_j)$ (with $j \neq 0$), and $\phi(\Lambda)$.

These relations are unproblematic for hyperbolic systems. In the nonhyperbolic case, instead, things are much less trivial, as illustrated on the examples of the logistic and Hénon maps. For instance, spectra of Liapunov exponents computed from periodic orbits do not coincide over the full range with those computed from randomly chosen aperiodic orbits. Not surprisingly, the above relations also have to be modified there. We claim that the needed modifications are, in some sense, minimal: they are *only* felt in the range of small Liapunov exponents, and only at small pointwise dimensions. While the periodic points are typical for the "normal" part of the spectrum and for a set of points of measure one on the attractor, the "exceptional" points are essentially those where the stable and unstable manifolds are tangent to each other.

This separation into two "phases" of points is clearly manifested as a singularity, similar to a first-order phase transition, in the generalized dimension function $D(q)$. For q below a critical value q_c, the normal (hyperbolic) points dominate, while above q_c the "phase" consists of the nonhyperbolic tangency points.

This interpretation is strongly suggested by the thermodynamic formalism involving, in particular, Legendre transforms between dimension functions ("free energies") and scaling functions ("internal energies"). What is still missing is a statistical mechanical treatment. In the analogy between dynamical systems and statistical mechanics, it is the members of a generating partition that correspond to the states of a spin in a one-dimensional lattice. Phase transitions in a one-dimensional spin model can only appear if there are either long-range forces or if the spin has infinitely many states. Translated into our present case, this means either that we must work with infinite partitions, if they should be Markov, or that there must be long-time correlations in the symbolic dynamics, if we work with simple (e.g., binary) partitions. As we said, we have not worked out any details.

ACKNOWLEDGMENT

We thank the IBM Zurich Research Laboratory for computational support.

REFERENCES

1. G. Parisi, Appendix, in U. Frisch, Fully developed turbulence and intermittency, in *Proceedings of International School on Turbulence and Predictability in Geophysical Fluid Dynamics and Climate Dynamics*, M. Ghil, ed. (North-Holland, 1984); U. Frisch, *Phys. Scripta* **T9**:137 (1985).
2. R. Benzi, G. Paladin, G. Parisi, and A. Vulpiani, *J. Phys. A* **17**:3521 (1984).
3. T. C. Halsey, M. H. Jensen, L. P. Kadanoff, I. Procaccia, and B. Shraiman, *Phys. Rev. A* **33**:1141 (1986); M. H. Jensen, L. P. Kadanoff, A. Libchaber, I. Procaccia, and J. Stavans, *Phys. Rev. Lett.* **55**:2798 (1985).
4. D. Ruelle, *Thermodynamic Formalism* (Addison-Wesley, Reading. Massachusetts, 1978); O. Lanford, Entropy and equilibrium states in classical and statistical mechanics, in *Statistical Mechanics and Mathematical Problems*, A. Lenard, ed. (Springer, 1976).
5. B. B. Mandelbrot, *The Fractal Geometry of Nature* (Freeman, San Francisco, 1982).
6. P. Grassberger, *Phys. Lett.* **97A**:227 (1983).
7. H. G. Hentschel and I. Procaccia, *Physica* **8D**:435 (1983).
8. P. Grassberger, *Phys. Lett.* **107A**:101 (1985).
9. V. N. Shtern, *Dokl. Akad. Nauk SSSR* **270**:582 (1983).
10. J.-P. Eckmann and D. Ruelle, *Rev. Mod. Phys.* **57**:617 (1985).
11. J. D. Farmer, E. Ott, and J. A. Yorke, *Physica* **7D**:153 (1983).
12. J.-P. Eckmann and I. Procaccia, *Phys. Rev. A* **34**:659 (1986); G. Paladin, L. Peliti, and A. Vulpiani, University of Rome, Preprint (1986).
13. V. Jakobson, *Commun. Math. Phys.* **81**:39 (1981); M. Misiurewicz, *Publ. Math. IHES* **53**:17 (1981).
14. M. Hénon, *Commun. Math. Phys.* **50**:69 (1976).
15. S. Newhouse, Lectures on dynamical systems, in *Dynamical Systems* (Birkhauser, Boston, 1980); J. Guckenheimer and P. Holmes, *Nonlinear Oscillations, Dynamical Systems and Bifurcations of Vector Fields* (Springer, New York, 1986).
16. E. Ott, W. Withers, and J. A. Yorke, *J. Stat. Phys.* **36**:687 (1984).
17. O. Rössler, *Phys. Lett.* **57A**:397 (1976); P. Holmes, *Phil. Trans. R. Soc. A* **292**:419 (1979).
18. A. Renyi, *Probability Theory* (North-Holland, Amsterdam, 1970).
19. R. Badii and A. Politi, *Phys. Rev. Lett.* **52**:1661 (1984); R. Badii and A. Politi, *J. Stat. Phys.* **40**:725 (1985).
20. L. P. Kadanoff, private communication.
21. J. Balatoni and A. Renyi, in *Selected Papers of A. Renyi*, Vol. 1, p. 558 (Akademia, Budapest, 1976).
22. S. J. Chang and P. R. Fendlay, *Phys. Rev. A* **33**:4092 (1986).
23. D. Rand, The singularity spectrum for hyperbolic cantor sets and attractors, University of Arizona, preprint (1986); P. Collet, J. Lebowitz, and A. Porzio, Dimension spectrum for some dynamical systems, to be published.
24. P. Fredrickson, J. L. Kaplan, E. D. Yorke, and J. A. Yorke, *J. Diff. Eqs.* **49**:185 (1983).
25. P. Grassberger, in *Chaos in Astrophysics*, J. Perdang *et al.*, eds. (Reidl, Dortrecht, 1985); P. Grassberger, in *Chaos*, A. V. Holden, ed. (Manchester University Press, Manchester, 1986).

26. P. Grassberger and I. Procaccia, *Physica* **13D**:34 (1984).
27. P. Billingsley, *Ergodic Theory and Information* (Wiley, New York, 1965).
28. F. Takens, Invariants related to dimension and entropy, in *Atas do 13° Coloquio Brasileiro de Matematica* (1984).
29. P. Grassberger and I. Procaccia, *Physica* **9D**:189 (1983).
30. J. D. Farmer, Order within chaos, Thesis, University of California, Santa Cruz (1981).
31. E. N. Lorenz, *Physica* **13D**:90 (1984); **17D**:279 (1985).
32. R. Badii and A. Politi, *Phys. Rev.* **35A**:1288 (1987).
33. H. Fujisaka, *Prog. Theor. Phys.* **70**:1264 (1983).
34. G. Györgyi and P. Szepfalusy, *Z. Phys. B* **55**:179 (1984); P. C. Hemmer, *J. Phys. A* **17**:L247 (1984); S. Grossmann and H. Horner, *Z. Phys. B* **60**:79 (1985).
35. B. V. Chirikov and D. L. Shepelyansky, *Physica* **13D**:395 (1984); P. Grassberger and H. Kantz, *Phys. Lett.* **113A**:167 (1985).
36. P. Grassberger, *Physica* **14D**:365 (1985).
37. F. Ledrappier and L. S. Young, *Ann. Math.* **122**:509 (1985).
38. Ya. B. Pesin, *Russ. Math. Surv.* **32**:55 (1977); D. Ruelle, *Ann. N. Y. Acad. Sci.* **136**:229 (1981).
39. R. Badii and A. Politi, *Phys. Scripta* **35**:243 (1987).
40. G. Julia, *J. Math. Ser. 7 (Paris)* **4**:47 (1918); P. Fatou, *Bull. Soc. Math. France* **47**:161 (1919); H. Brolin, *Ark. Mat.* **6**:103 (1965).
41. D. Ruelle, *Ergod. Theory Dyn. Syst.* **2**:109 (1982); A. Manning, University of Warwick preprint (1984).
42. S. Ulam and J. Von Neumann, *Bull. Am. Math. Soc.* **53**:1120 (1947).
43. L. de Arcangelis, S. Redner, and A. Coniglio, *Phys. Rev. B* **31**:4725 (1985); R. Rammal, C. Tannous, and A.-M. S. Tremblay, *Phys. Rev. A* **31**:2662 (1985).
44. S. Roux and C. D. Mitescu, *Phys. Rev. B* **35**:898 (1987).
45. P. Cvitanovic, unpublished notes.
46. R. Gonczi, Evaluation of the capacity of a strange attractor by a discretization method, University of Nice preprint (1986).
47. P. Grassberger, *Phys. Lett.* **97A**:224 (1983).
48. W. E. Caswell and J. A. Yorke, in *Dimensions and Entropies in Chaotic Systems*, G. Mayer-Kress, ed. (Springer, Berlin, 1986).